

Ease-of-use

The new, groundbreaking
LC-technology: Nexera LC-40

Searching for the needle in
the analytical haystack

Trace detection of sulfur
compounds with SCD

20 Years

Shimadzu Switzerland
celebrates anniversary



APPLICATION

- Scents and sensitivity – LRI in LC: reliable characterization of oxygen heterocyclic compounds in citrus essences 4
- Not all glass is the same – Quality control of window glass according to DIN EN 410 7
- Extending GCMS to the analysis of Active Pharmaceutical Ingredients 10
- Everything styrene? Identification of plastics in recycling 14
- What a smell! Identification of pyrazines and methional by heart-cut GC-O/GC-O/MS 22
- Monitoring of total aromatics in gasoline – GCMS-QP2020 applied to ASTM D5769-04 25
- The glowing lemonade – Fluorescence analysis of quinine flavor in various preparations 30

PRODUCTS

- Groundbreaking LC technology – The new Nexera LC-40 series merges ease-of-use and peace-of-mind 12
- Safety first – well protected with guard columns 18
- Searching for the needle in the analytical haystack – Trace detection of sulfur compounds with SCD 28

LATEST NEWS

- Shimadzu Switzerland celebrates its 20th anniversary 2
- Recognized for outstanding designs – iF DESIGN AWARD 2019 32

MARKETS

-  Chemical, Petrochemical, Biofuel and Energy
-  Clinical
-  Environment
-  Food, Beverages, Agriculture
-  Pharmaceutical
-  Plastics and Rubber
-  Automotive

Facing the Swiss market

Shimadzu Switzerland celebrates its 20th anniversary



Team artwork »Made by Individuals« for the 20th anniversary, 2019



A small office space in the industrial park of Reinach, Switzerland and two employment ads in the local newspaper: these were the beginnings of Shimadzu Schweiz GmbH. In 1999, Shimadzu Europa sent a representative to Switzerland to develop the market for the company. On February 18, the same year Shimadzu Switzerland was officially entered in the commercial register. This was the cornerstone for a promising future.

The location of the subsidiary has been chosen strategically. It is located in the outskirts of Basel where the Swiss, French and German borders meet. This area is one of the most dynamic economic regions of Switzerland. Pharmaceuticals and specialty chemicals have become the

modern focus of the city's industrial production.

Shimadzu Switzerland is one of ten independent subsidiaries in Shimadzu's network of branch and distribution offices all over Europe. This status enables more freedom to better adjust business processes to customer requirements and markets, and to

respond to local cultural conditions and traditions.

From start-up to SME

With only five people, Shimadzu Switzerland was a start-up company, which was also reflected in the day-to-day work routine. The first employee was recruited in May 1999 for the back office,



Carméla Meisenbach, Open days Office Reinach, 2000



Current group photo, Bad Ramsach Läuelfingen, 2018

soon followed by the first service technician and a second clerk. The fifth person was responsible for sales (E. Pelosi, U. Gschwind and Ch. Marx are still engaged at Shimadzu Schweiz.). After a short time, the first office was already too small, and the crew moved to the present location in Römerstrasse 3. The new location was inaugurated in 2000 with an open house.

After the initial challenges, procedures and tasks were shaped and trimmed over time, and are still fine-tuned today according to customer needs. In 2007, a major step forward was the introduction of a new software for enterprise resource planning purposes. It streamlines processes, provides deeper insights and professionalizes the workflow, thus making Shimadzu more efficient as an organization.

ILMAC – important as a market forum

In 2005, Shimadzu Switzerland participated for the first time in the ILMAC show in Basel in order to increase its brand awareness and to be recognized as a player in the industry. To date, this show for process and laboratory technology is one of the most

important exhibitions for the subsidiary. It is where innovations are exhibited, customer contacts are maintained and new relationships are established.

Shimadzu's first ILMAC stand was located under the escalators, a draughty corner leaving some employees with stiff necks after the fair. Meanwhile, Shimadzu Switzerland owns one of the largest booths, E201, in the main hall. The 20-year anniversary will be celebrated here in September 2019 with various attractions. All stakeholders are welcome to visit Shimadzu during these days.

Basis for stability and security as well as growth and success

To date, Shimadzu Switzerland has grown to the size of a medium-sized SME. Qualified sales and service engineers, application chemists and the powerful internal sales team together form a well-functioning unit. They are

20th anniversary celebration, Binningen Castle, 2019

Action Painting, 2019

Shimadzu's face to the customers on the Swiss market.

Since the beginning, much has changed in technical, organizational and staffing terms. The strength of Shimadzu Switzerland is the constellation of experienced and young employees. Experienced people train the younger generation, while on the other hand new talents bring in new ideas, tools and networks. The

employees transfer their special work atmosphere and positive mood to customers, while Shimadzu gauges customer feedback and reactions to steadily increase performance.

For two decades, customers in Switzerland have relied on Shimadzu as their market partner, and the 360 degree service is guaranteed – innovative, adaptable and trustworthy. Shimadzu Switzerland will ensure that this balance always remains as a basis for stability and security as well as growth and success.



Scents and sensitivity

LRI in LC: reliable characterization of oxygen heterocyclic compounds in citrus essences

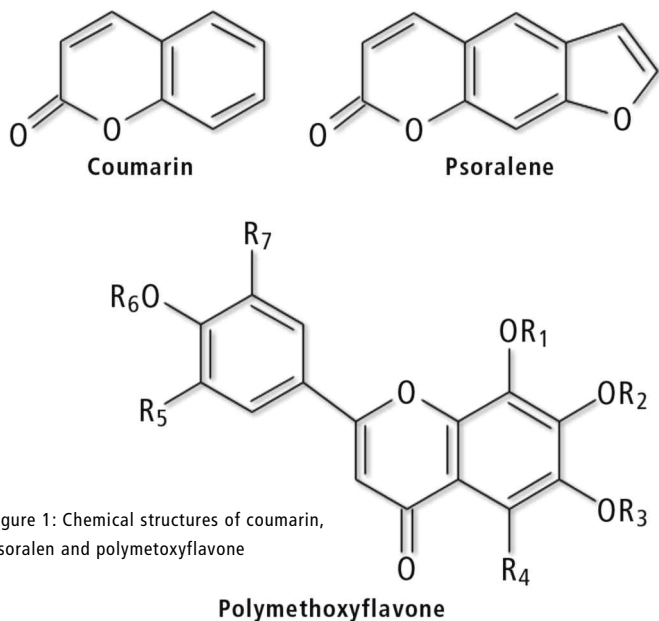


Figure 1: Chemical structures of coumarin, psoralen and polymethoxyflavone

Citrus fragrances are highly appreciated in cosmetics as they provide a fresh and invigorating odor. Coumarins (C), furocoumarins (FC), also called psoralens, and polymethoxyflavones (PMF) (figure 1), commonly named oxygen heterocyclic compounds (OHC) are molecules naturally contained in citrus essence, widely used in the cosmetic industry. These compounds are part of many cosmetic products of both leave-on and rinse-off types.

Furocoumarins, for example, are produced by a variety of plants such as bergamot, lemon, lime, and grapefruit. However, FCs acquire phototoxic effects after exposure to sunlight, so their maximum amount in cosmetics is restricted by the European Parliament through the Regulation (EC) No. 1223/2009 [1] and subject to opinions from several associations.

Although many advanced analytical strategies are available to char-

acterize the non-volatile fractions of citrus oils in order to evaluate their authenticity and content of OHC, liquid chromatography (LC) coupled to photodiode array detector (PDA) is still the most widely used method by the majority of companies. The reasons why this technique is so widely employed are limited instrumentation costs and easy applicability, being suitable for routine quality control processes.

Correct determination of the non-volatile fraction of citrus oils is very important for the cosmetic industry, because it provides the quantitative information needed in order to combine essences without exceeding the official limits. In fact, citrus oils are often subjected to distillation or other processes to reduce the content of psoralens.

Despite wide knowledge about the applicability of the HPLC-PDA method for analysis of essences, a recent work by the International Fragrance Association (IFRA)

focused on the limitations of PDA detection in the determination of FC in cold pressed citrus essential oils. The authors fixed the limit of quantification (LOQ) of 15 target FCs at 10 mg/L due to the low selectivity and sensitivity of PDA detection [2].

Proper strategy for identification and quantification of FCs

It must be admitted that PDA detection is less selective when compared to other detection approaches, but FCs have characteristic UV-Vis spectra and can be

correctly identified and quantified using PDA by applying a proper strategy. The strategy reported here addresses the Linear Retention Index (LRI) system as an extra criterion for identification in combination with the UV-Vis library; just as in GC where identification is based on spectral similarity (EI-MS) and the LRI filter.

The LRI parameter correlates retention time of the targets with a reference standard mixture. In this way, by the injection of a suitable homologous series of standards, a specific LRI value will be attributed to the analytes [3].



Figure 2: UHPLC Nexera-i system

Automatic identification by the software, based on spectra similarity, is subject to restriction of the LRI range, which guarantees unequivocal identification.

If more candidates are suggested due to high match with the library, the LRI provides the information based on retention behavior to restrict identification to just one candidate.

The chromatographic system of choice

One of the reasons why the LRI system has been limited in LC is the low reproducibility of older instrumentation, which was responsible for differences in the flow rate and elution gradient also between consecutive analyses.

In this context, the UHPLC Nexera-i (figure 2, page 6) represents the chromatographic system of choice to apply this strategy. Thanks to its robustness, this instrument has all the characteristics needed to guarantee the stability of the LRI approach. Nexera-i also ensures automation of many routine analyses, exactly what is required by companies to achieve rapid and reliable results and proper data elaboration in quality control.

LRI, calibration curves and UV-Vis library were obtained by the analysis of 35 standard compounds, among them FC, C and PMF, under the HPLC-PDA conditions described in table 1 (page 6) [4]. For calculation of LRI, the homologous series of alkyl aryl ketones (from C8 to C13) was selected based on its wide range of retention times, suitable to cover the chromatographic window of all targets, and for the capability of these molecules to absorb at 254 nm.

Calibration curves and library

Calibration curves were generated in two ways: in pure solvent and in three different distilled essential oils used as blank samples to evaluate matrix effects and provide correct LOQ. The lowest linear points of the curves on blanks were considered the LOQ, being

the lowest concentration not affected by the matrix.

Spectra of the targets, injected in pure solvent, were collected to create the library. In less than 10 min all standards were separated. Figure 3 shows the automatic calculation of LRI by LabSolutions software version 5.85, referring to the corresponding analysis of the alkyl aryl ketones. The manual equivalent operation to obtain LRI would use the equation developed by van den Dool and Kratz [4]. The applicability of the LRI system in LC was possible thanks to the robustness of the Nexera-i system. The high repeatability in terms of retention times is reported in figure 4 (page 6).

The UV-Vis library consists of 35 spectra, acquired in the range 190-370 nm, of 19 FC, 8 C and 7 PMF. In most cases the library was able to provide one candidate (figure 5, page 6), however in some cases LRI plays a key role in correct identification. This demonstrates how the combination of library and LRI overcomes the low selectivity of PDA detection, for discrimination of molecules with very similar spectra.

Cold pressed citrus essential oils: correct quantitative determination of FC

The second focus of the study was to limit the interference of matrix effects in order to achieve correct quantitative determination of FC in cold pressed citrus essential oils. The calibration curves constructed on distilled citrus oils demonstrated how to avoid overestimation. LOQ, established as the lowest linear points of the curves, always resulted in much lower values than those suggested by IFRA. In particular, each molecule gave a specific LOQ depending on the distilled oil used as matrix and consequently on the presence of specific co-eluted interfering compounds. For FC, these limits were equal to 0.1 or 0.5 mg/L for almost all compounds, considering the distilled oils used (bergamot, lemon and mandarin). ♦

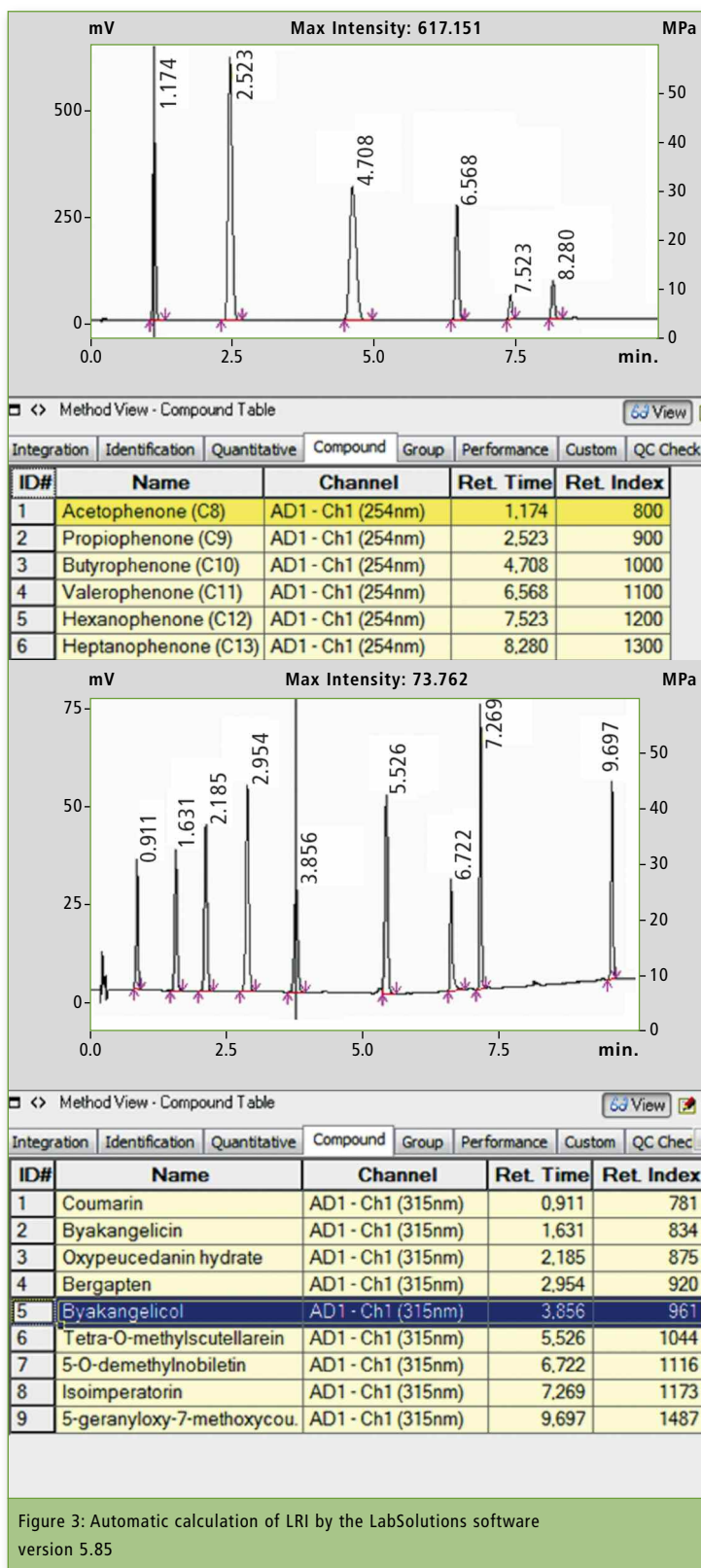


Figure 3: Automatic calculation of LRI by the LabSolutions software version 5.85

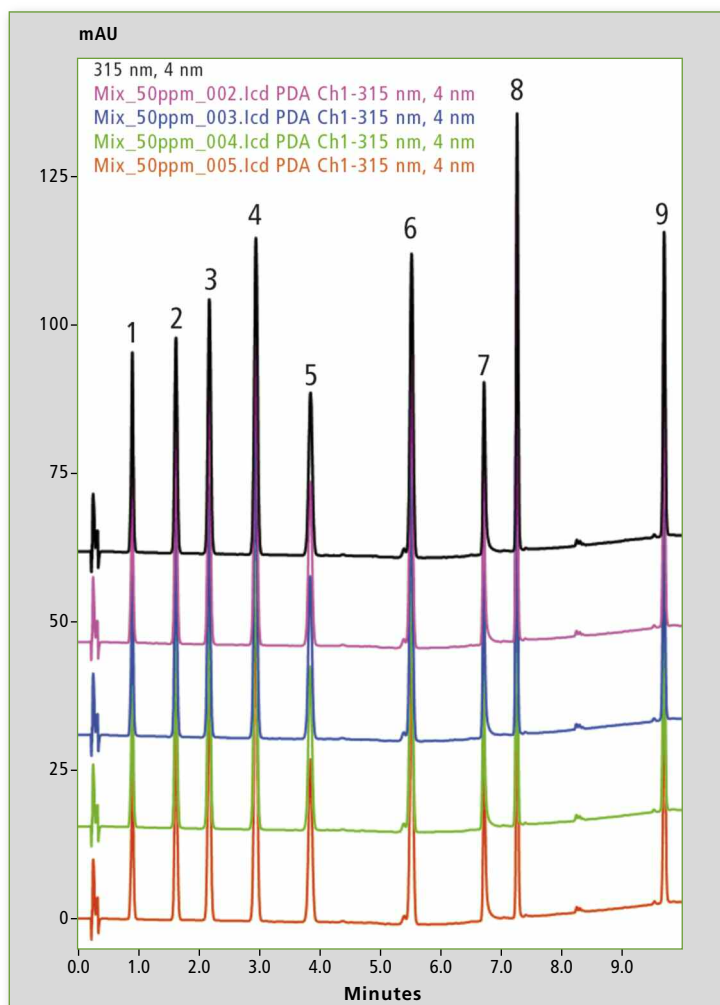


Figure 4: Retention time repeatability of a mixture of standards analyzed using the Nexera-i system. 1. Coumarin (I.S.), 2. Byakangelicin, 3. Oxypeucedanin hydrate, 4. Bergapten, 5. Byakangelicol, 6. Tetra-O-methylscutellarein, 7. 5-O-demethylnobiletin, 8. Isoimperatorin, 9. 5-geranyloxy-7-methoxycoumarin.

Conclusion

Both strategies adopted LRI approach and calibration curves on blanks, demonstrated to enable a correct characterization of FC, C and PMF in citrus cold pressed essential oils.

The Nexera-i system confirms its suitability as the instrument of choice for this type of application. The robustness of the system makes the LRI approach perfectly applicable. Due to its ease of use, the Nexera-i system is suitable for QC of essential oils and many other samples.

The method was used to characterize OHC in different cold pressed citrus oils. Calibration curves on blanks provided accu-

rate results: in fact, the amounts calculated were always lower than the data obtained with calibration curves in pure solvent.

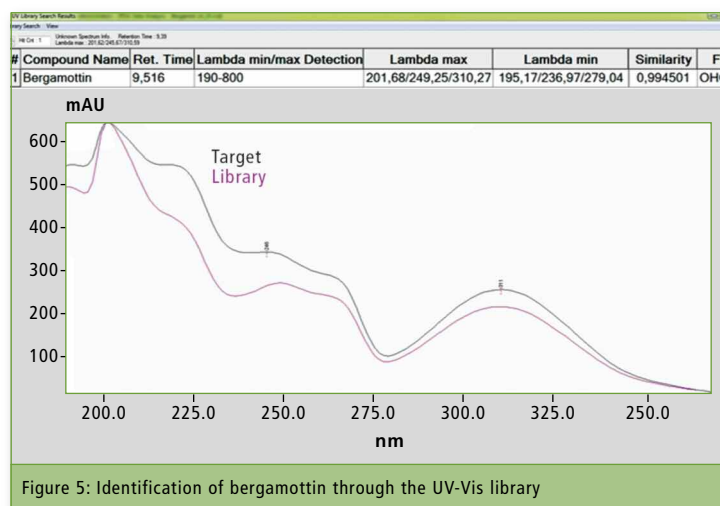


Figure 5: Identification of bergamottin through the UV-Vis library

Column	Ascentis Express C ₁₈ column (50 x 4.6 mm, 2.7 μm)*
Solvent A	water/methanol/THF (85:10:5 v/v)*
Solvent B	methanol/THF (95:5 v/v)*
Elution gradient	0 min, 15% B; 4.5 min, 28% B, 7 min = 60% B, 11 min = 85% B, 14 min = 85% B
Flow rate	2 mL/min
Oven temp.	40 °C
Injection vol.	2 μL
PDA	4.1667 Hz, time constant 0.480 sec, wavelength range 190 - 370 nm. OHC chromatogram extracted at 315 nm. Homologous series chromatogram extracted at 254 nm.

Table 1: HPLC-PDA analysis conditions.

*Merck Life Science (Merck KGaA, Darmstadt, Germany).

The application of LRI in LC was the main challenge of this research and showed its validity and applicability for reliable identification of OHC, especially FC, even at concentrations lower than 10 mg/L.

The method was also applied to a Nexera UHPLC instrument coupled to an LCMS-8060 for calculation of LRI. The results were absolutely comparable, and underline the concept of applicability of LRI in liquid chromatography.

Next step will be the application of this analytical approach to other matrices, for instance food, due to the increase of scientific articles focussing on evaluation of harmful effects on human health as consequence of furocoumarin dietary intake.

Authors

Adriana Arigò¹, Francesca Rigano², Paola Dugo^{1,2,3} and Luigi Mondello^{1,2,3,4}

¹ Department of Chemical, Biological, Pharmaceutical and Environmental Sciences, University of Messina, Italy

² Chromaleont S.r.l. c/o Department of Chemical, Biological, Pharmaceutical and Environmental Sciences, University of Messina, Italy

³ Unit of Food Science and Nutrition, Department of Medicine, University Campus Bio-Medico of Rome, Italy

⁴ BeSep S.r.l. c/o Department of Chemical, Biological, Pharmaceutical and Environmental Sciences, University of Messina, Italy

Literature

- [1] European Parliament, Official Journal of the European Union, L 342 (2009) 59, 22.12.2009. Regulation (EC) No 1223/2009 of the European Parliament and of the Council of 30 November 2009 on cosmetic products (recast) (Text with EEA relevance). <https://eur-lex.europa.eu>
- [2] Macmaster, A.P. et al. Quantification of selected furocoumarins by high performance liquid chromatography and UV-detection: capabilities and limits. *J Chromatogr. A.* 2012;1257:34-40.
- [3] van den Dool, H. and Kratz, P.D. A Generalization of the Retention Index System Including Linear Temperature Programmed Gas-Liquid Partition Chromatography. *J Chromatogr.* 1963;11: 463-471.
- [4] Russo, M. et al. Reduced time HPLC analyses for fast quality control of citrus essential oils. *J Essen Oil Res.* 2015;4: 307-315.



Not all glass is the same

Quality control of window glass according to DIN EN 410



Construction thermography: surfaces with increased heat dissipation are marked in red

Windows, glass roofs, conservatories – glass is not only an important building material, but also an architectural element. It shapes surfaces, and modern glasses can even take on static functions. A smartly selected glazing is an important contribution to the effective thermal insulation of a building. It is therefore essential for builders to be able to compare materials based on defined characteristics. For glass and similar building materials, they are defined primarily for the European market in DIN EN 410.

Samples and measurement setup

Shimadzu studied six samples of uncoated soda-lime glass (figure 1) for use in construction. This clear or colored glass can be used both indoors and outdoors. All samples were produced using the float glass process and differ only in their layer thickness. Float glass is the most common type of glass today and is produced in a long, steady flow.

The spectra required to calculate the characteristics were recorded using a Shimadzu UV-3600 Plus spectrophotometer with ISR-1503F integrating sphere. This integration sphere has a diameter of 150 mm and three detectors (photomultiplier, InGaAs, PbS) to cover the entire DIN-compliant measuring range of 300 - 2,500 nm.

The hollow integrating sphere is coated on the inside with a highly reflective material. In the case of the ISR-1503F, Spectralon®, a polymer of fluorine and carbon, is used. Diffused light scattered into the sphere is reflected on the walls until it hits one of the three detectors. For evaluation according to DIN EN 410, the glass sample is measured once in diffuse transmittance mode and once in diffuse reflection mode (8° angle of incidence). The different measurement configurations are shown in figure 2. ▶

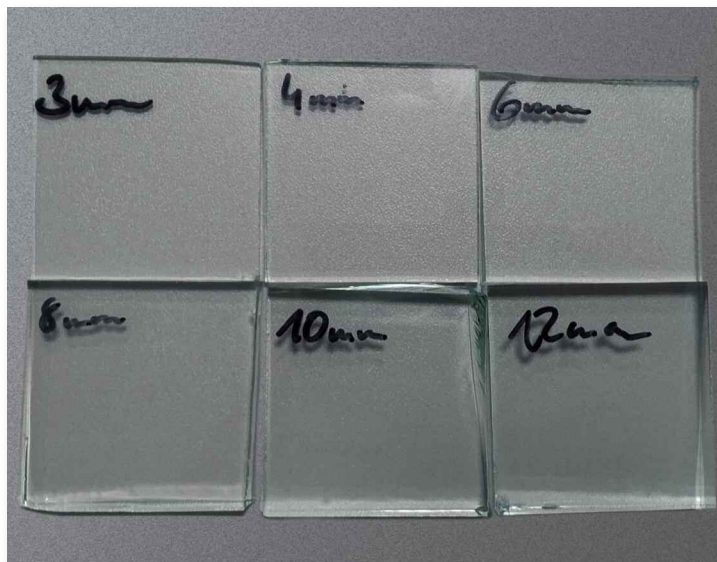
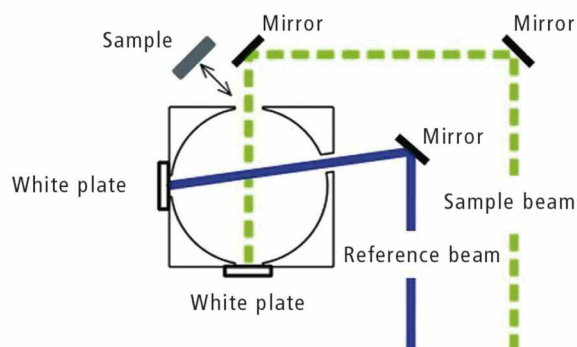


Figure 1: Examined glass samples. From top left to bottom right: 3, 4, 6, 8, 10 and 12 mm thickness uncoated soda-lime float glass.

Transmission Measurement:



Reflection Measurement:

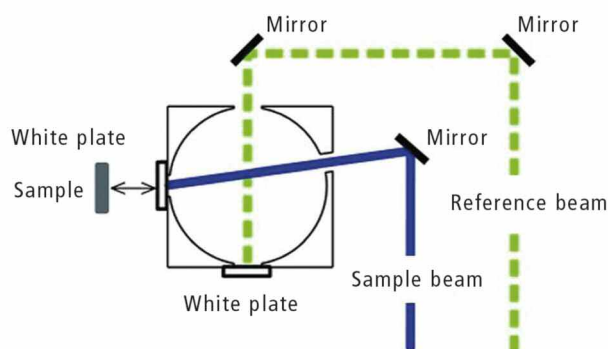


Figure 2: Measurement configurations with the integrating sphere. The diagram shows the side view with the device front facing left. Irradiation with 8° incidence angle also reflects the directionally reflected light on the inner wall of the sphere and not towards the entrance aperture.

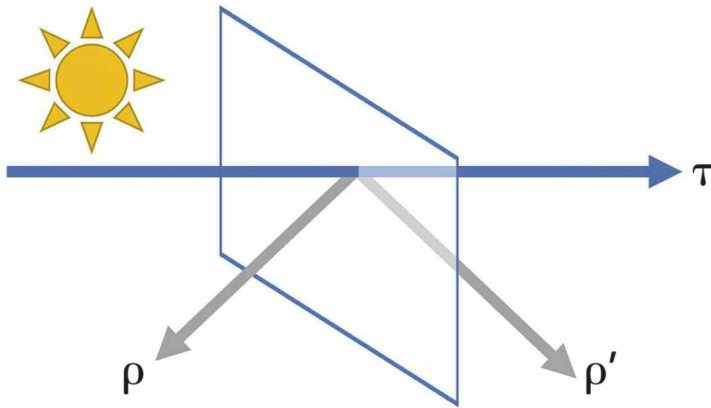


Figure 3: Photometric characteristics of a single glazing: transmittance τ through the pane, reflectance ρ on the outside and reflectance ρ' on the inside.

Definitions of the characteristics

The characteristics defined in DIN EN 410 are referred to in figures 3 and 4. Here, only the calculations for uncoated, single glazing are discussed.

The starting points for all calculations are measurement of transmittance through the sample and reflectance from each sample side. For coated glass, the transmittance may vary depending on the side, so whichever side of the built-in window is the inside and which is the outside must be defined.

The characteristics are:

- Spectral transmittance $\tau(\lambda)$ and spectral reflectance $\rho(\lambda)$ in the wavelength range from 300 nm to 2,500 nm.
- Light transmittance τ_v and light reflectance ρ_v for standard illuminant D65. [5]
- Solar direct transmittance τ_e and solar direct reflectance ρ_e normalized to the relative spectral distribution of solar radiation. [6]
- Solar factor g .
- UV transmittance τ_{UV} normalized to the relative spectral distribution of the UV range of global radiation. [7]
- General color rendering index R_a .
- Shading coefficient SC.

The transmittance and reflectance values ($\tau[\lambda]$, $\rho[\lambda]$) measured for individual panes are used to calcu-

late the purely photometric characteristics τ_v , ρ_v , τ_e , ρ_e and τ_{UV} according to equation 1 with tabulated normalization factors.

$$x_i = \frac{\sum_{\lambda} N(\lambda) \cdot M(\lambda)}{\sum_{\lambda} N(\lambda)}$$

Equation 1: Generalized form of the equations describing single glazing with λ as wavelength in nanometers, x_i as characteristic, $N(\lambda)$ as normalization factor and $M(\lambda)$ as measured value (transmittance or reflectance). The limits of the sum and the scaling factor depend

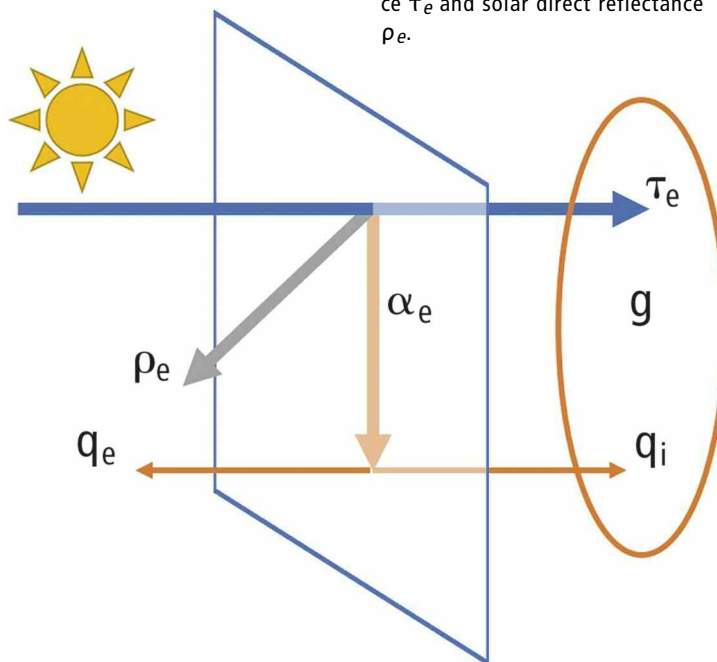


Figure 4: Radiation-physical characteristics of a single glazing: Direct solar absorptance α_e , secondary external heat transfer factor q_e , secondary internal heat transfer factor q_i and solar factor g as the product of τ_e and q_i .

on the respective parameter and are tabulated in DIN EN 410.

In addition, the general color rendering index R_a is calculated from the transmittance spectrum in the visible range and the values for defined test colors tabulated in DIN EN 410. It describes how much the color perception is influenced by the glass.

For multiple glazing, internal reflectance between the panes must be included for all calculations. In this case, the spectra of the panes used are first measured individually. $\tau(\lambda)$ and $\rho(\lambda)$ are then calculated from these individual spectra for the whole system.

From τ_e and ρ_e , further characteristics are determined which are shown in figure 4 and describe the thermal properties of the glazing. The solar direct absorptance α_e is the part of the solar radiation that is absorbed by the glass according to equation 2.

$$\alpha_e = 1 - \tau_e - \rho_e$$

Equation 2: Direct solar absorptance α_e with solar direct transmittance τ_e and solar direct reflectance ρ_e .

The energy absorbed is converted by the glass into heat and discharged to the inside and to the outside in the form of the secondary external (q_e) and internal (q_i) heat transfer factor. The calculation of the solar factor g for single glazing with uncoated soda-lime glass can be summarized in equation 3.

$$g = \tau_e \cdot q_i = \tau_e \cdot 0.24 \cdot \alpha_e$$

Equation 3: Simplified formula for calculating the solar factor g . For multiple glazing, q_i must be calculated using the thermal conductivity of the gas gap.

For this special case, calculation of the thermal transmittance U_g of the glazing can be summed up as a function of the glass thickness according to equation 4.

$$U_g = x \cdot 1.17 \text{ m}^{-1}$$

Equation 4: Simplified formula for calculating the thermal transmittance U_g from the glass thickness in meters. In the case of multiple glazing, additional thickness and thermal conductivity of the gas interlayers must be included.

Finally, from g according to equation 5, the shading coefficient SC is calculated. For multiple glazing, the thermal conductivity of the gas gap must be included. The corresponding calculations are given in DIN EN 673. Depending on the material or coating, it may also be necessary to determine the corrected emissivity of each single pane from FTIR spectra according to DIN EN 12898.

$$SC = \frac{g}{0.87}$$

Equation 5: Shading coefficient SC according to DIN EN 410.

Measurement results

Transmittance and reflectance spectra of the samples displayed in figure 1 (page 7) in the range of 300 - 2,500 nm are shown in figure 5. The characteristics calculated from these spectra are given in

Parameters	Unit	3 mm	4 mm	6 mm	8 mm	10 mm	12 mm
Thermal transmittance, U_g	$\frac{W}{m^2 K}$	5.78	5.75	5.69	5.62	5.56	5.50
Solar factor, g	%	88.03	87.17	84.94	83.42	81.21	78.93
Light transmittance, τ_v	%	90.36	90.11	89.43	88.76	88.18	86.91
Light reflectance, ρ_v	%	8.83	8.97	8.91	9.10	8.76	8.42
Solar direct transmittance, τ_e	%	86.92	85.79	82.79	80.80	77.74	74.59
Solar direct reflectance, ρ_e	%	8.51	8.51	8.34	8.44	7.96	7.54
Solar direct absorptance, α_e	%	4.57	5.70	8.87	10.75	14.30	17.88
Secondary internal heat transfer factor, q_i	%	1.11	1.38	2.15	2.61	3.47	4.34
Ultraviolet transmittance, τ_{UV}	%	70.64	69.93	64.78	61.07	57.40	53.47
Shading coefficient, SC	%	101.19	100.20	97.64	95.88	93.35	90.72
General color rendering index, R_a		98.71	98.52	97.99	97.66	97.03	96.45

Table 1: Characteristics of the samples evaluated, as calculated from the transmittance and reflectance spectra shown in figure 5 and the formulae and constants given in DIN EN 410.

table 1. For the calculation, a commercial spreadsheet software was used.

As can be seen in table 1, the glass thickness has little effect on the thermal transmittance U_g . Therefore, heat-insulating glazing is achieved by multiple glazing of thin panes (3 - 4 mm) with insulating gas intermediate layers. Additional thermal insulation can be achieved if the outermost pane is provided with a coating which

reflects infrared radiation to the outside.

All transmittance and reflectance values of the samples examined here decrease with greater thickness, especially in the UV range. However, the solar direct absorptance and the secondary internal heat transfer factor increase accordingly. Nevertheless, as part of the heat is released to the outside, the overall energy transmittance decreases slightly.

With these almost colorless types of glass, the color rendering index is hardly influenced by the glass thickness.

Conclusion

The characteristics defined in DIN EN 410 are important quality features of glazing for different purposes. The material thickness plays only a minor role for the calculated characteristics. To determine the characteristics for the starting material of a glazing, a UV-Vis-NIR spectrophotometer with an integration sphere is required, such as the Shimadzu UV-3600 Plus with ISR-1503. For the assessment of multiple glazing, the properties of the intermediate layers must also be known.

Literature

- [1] DIN EN 410:2011, Glass in Building – Determination of Luminous and Solar Characteristics of Glazing, German Version EN 410:2011
- [2] DIN EN 673:2011, Glass in building – Determination of thermal transmittance (U value) – Calculation method; German version EN 673:2011
- [3] DIN EN 12898:2001-04, Glass in building – Determination of the emissivity; German version EN 12898:2001
- [4] CIE No. 15, Colorimetry, 3. Edition (2004)
- [5] CIE No. 85, Solar spectral irradiance, technical report (1989)
- [6] P. Bener, Approximate values of intensity of natural UV radiation for different amounts of atmospheric ozone, Final Technical Report 1972, Contract No. DAJA 37-68 C-1077

Further information on this article:

- Application: Glass Plate Analysis in Accordance with DIN EN 410 Part 1

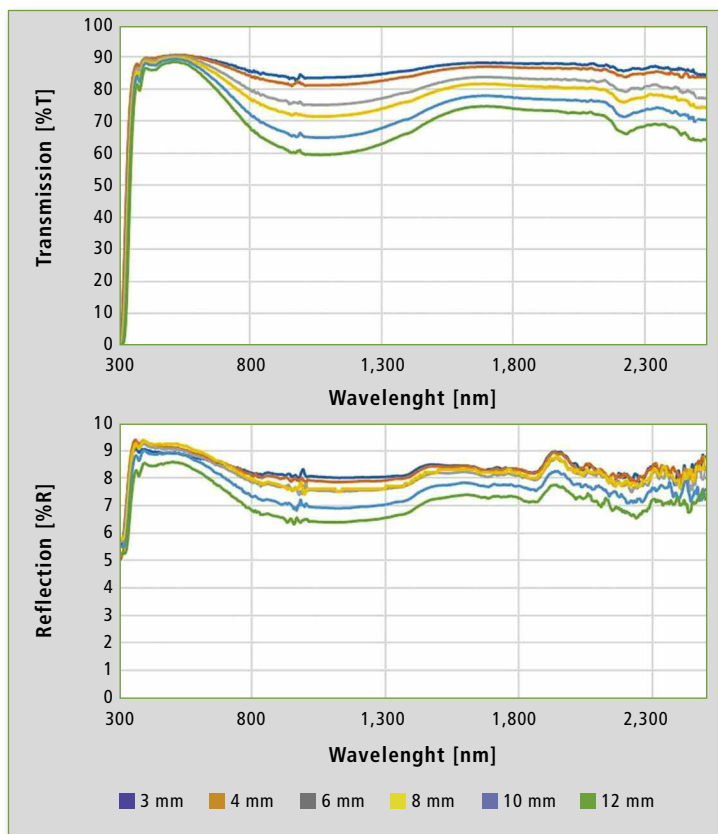


Figure 5: Transmittance spectra (top) and reflectance spectra (bottom) of the six glass samples shown in figure 1 in the spectral range from 300 to 2,500 nm

IMPRINT

Shimadzu NEWS, Customer Magazine of Shimadzu Europa GmbH, Duisburg

Publisher

Shimadzu Europa GmbH
Albert-Hahn-Str. 6-10 · D-47269 Duisburg
Phone: +49-203-76 87-0
Fax: +49-203-76 66 25
shimadzu@shimadzu.eu
www.shimadzu.eu

Editorial Team

Uta Steeger
Phone: +49 (0)203 76 87-410
Ralf Weber, Maximilian Schulze

Design and Production

m/e brand communication GmbH GWA
Duesseldorf

Circulation

German: 5,350 · English: 4,535

Copyright

Shimadzu Europa GmbH, Duisburg, Germany – July 2019.

Windows is a trademark of Microsoft Corporation. ©2019

Apple Inc. All rights reserved. Apple, the Apple logo, Mac OS and iOS are trademarks of Apple Inc.



Extending GCMS to the analysis of Active Pharmaceutical Ingredients

Analysis of N-Nitrosodimethylamine (NDMA) and N-Nitrosodiethylamine (NDEA) in pharmaceutical substances by HS-GCMS



Headspace-Autosampler HS-20

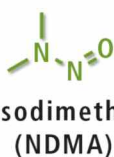
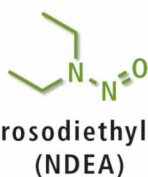


Figure 1: Structure of NDEA and NDMA

N-Nitrosodimethylamine (NDMA) and N-Nitrosodiethylamine (NDEA) are the simplest dialkyl nitrosamines. They continue to be released as a by-product and contaminant from various industries and from municipal wastewater treatment plants. Major releases of NDMA and NDEA are caused by the manufacture of pesticides, rubber tires, alkyl amines and dyes. These compounds are also produced as a by-product in the

manufacture of Active Pharmaceutical Ingredients (API's). These compounds are classified as a Group 2A carcinogen (probable human carcinogen) by the World Health Organization.

Recently, some drug products were discovered to have been contaminated with NDMA and NDEA (figure 1). It is believed that they were introduced into the finished products during the manufacturing process. The contami-

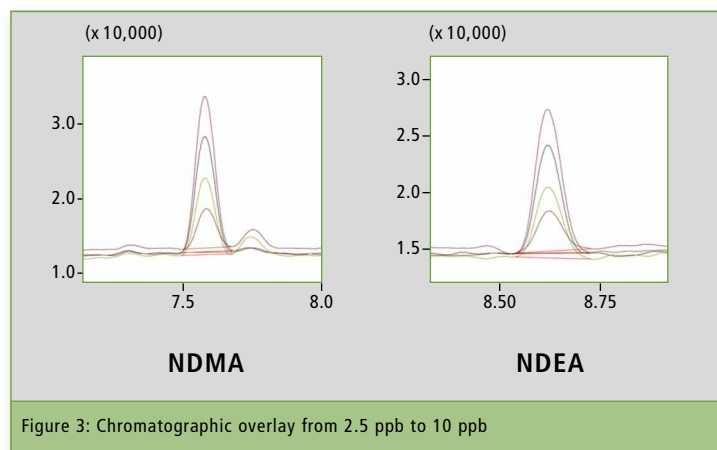
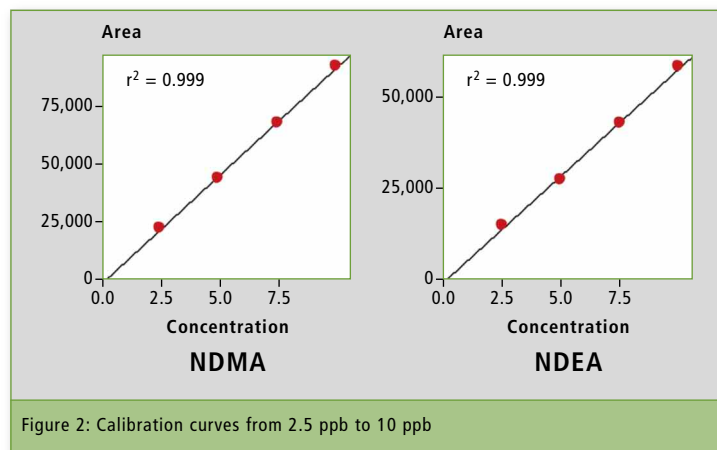
nation exceeded by far the regulatory exposure limits specific to the drug products. Consequently, medical agencies across Europe as well as the US Food and Drug Administration (USFDA) withdrew all affected drug products from the market.

It is therefore essential to have a sensitive, accurate, reliable and robust analytical method available based on a suitable technique. A Headspace Gas Chromato-

graphy Mass Spectrometry (HS-GCMS) method has been developed to detect the presence of NDMA in drug substances. In this experiment, the pharmaceutical API's (Valsartan, Losartan and Olmesartan-Medoxomil) subject to contamination with NDMA and NDEA are analyzed.

Experimental

This study was conducted using a Shimadzu GCMS-QP2020 NX



single quadrupole with HS-20. A commercial mixture of NDMA and NDEA was used to prepare calibration curves ranging from 2.5 - 10 µg/L. The standards were prepared in N,N-Dimethyl sulfoxide. Instrument operating conditions are shown in table 1.

Linearity of the calibration curve

A four-point calibration curve of NDMA and NDEA from 2.5 to 10 µg/L was analyzed using the conditions described in table 1. Retention times, correlation coefficient and LOQ (limit of quantification) established from S/N (signal/noise) and % RSD (relative standard deviation) are shown in table 2. The calibration curves established for both components with r^2 greater than 0.999 for calibration levels 2.5, 5.0, 7.5 and 10.0 ppb are shown in figure 2. Figures 3 and 4 depict chromatographic overlay of all linearity levels and six replicates of 5.0 ppb solution respectively.

Sample analysis and recovery test

Three API samples (Valsartan, Losartan & Olmesartan-Medoxomil) were weighed individually in a 20 mL headspace vial, to which 2 mL of DMSO were added as diluent to make 5 % w/v (weight/volume) solution. For the recovery tests, individual APIs were weighed in 20 mL headspace vials which were spiked with 2 mL 2.5 ppb, 5.0 ppb and 10.0 ppb NDMA and NDEA standard solutions respectively, and were then subjected to HS-GCMS analysis. Tables 3 and 4 show results of the sample analysis and accuracy study for 3 API's.

Conclusion

- A highly sensitive method was developed for quantitation of genotoxic impurities namely NDMA and NDEA in pharmaceutical API's using Shimadzu's GCMS QP2020 NX with HS-20 headspace autosampler.
- The SIM method developed can be used for screening of NDMA and NDEA in various pharmaceutical products.

Instrument details		Shimadzu GCMS-QP2020 NX with HS-20	
GC parameters			
Column	SH-Stabilwax, 30 m, 0.32 mm ID, 0.25 µm df		
Injection mode	Splittless		
Flow control mode	Linear velocity		
Carrier gas	Helium		
Column flow	1.60 mL/min		
Linear velocity	45.6 cm/sec		
Temperature program	40 °C (2 min) → (10 °C/min) → 120 °C → (25 °C/min) → 230 °C (5.6 min)		
HS-20 parameters			
Mode	Loop (1 mL)		
Oven temperature	120 °C		
Sample line temperature	125 °C		
Transfer line temperature	130 °C		
Equilibrating time	15.0 min		
MS Parameters			
Ion source temperature	200 °C		
Ionization mode	EI		
Mode	SIM		
	NDMA	NDEA	
	74, 42 & 43	102, 57, 56 & 44	
Electron voltage	70 eV	70 eV	

Table 1: GCMS-QP2020 NX operating conditions

Component	R.T. [min]	LOQ (2.5 ppb)		r^2
		S/N	% RSD	
NDMA	7.58	134	4.0	0.999
NDEA	8.63	118	8.2	0.999

Table 2: LOQ summary

Found component amount [ppb]	API		
	Valsartan	Losartan	Olmesartan-Medoxomil
NDMA [ppb]	Not detected	Not detected	Not detected
NDEA [ppb]	130.4	74.1	Not detected

Table 3: Results obtained by sample analysis

Concentration	API					
	Valsartan % Recovery		Losartan % Recovery		Olmesartan-Medoxomil % Recovery	
	NDMA	NDEA	NDMA	NDEA	NDMA	NDEA
2.5 ppb	108.6	104.6	95.0	113.4	103.4	114.4
5.0 ppb	99.9	96.5	96.1	107.9	89.8	88.7
10.0 ppb	114.2	114.2	99.8	107.7	98.3	102.7

Table 4: Results obtained in the accuracy study for three API's

- Ultra-Fast scanning and ASSP™ (Advanced Scan Speed Protocol) features of Shimadzu GCMS enabled a sensitive, selective, fast, reproducible and linear method of analysis.

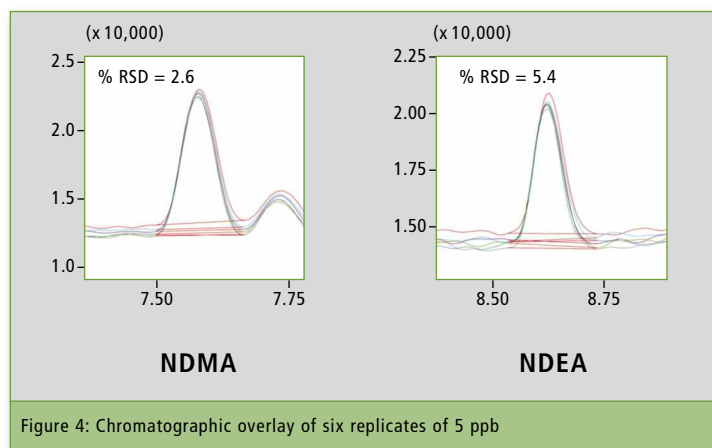


Figure 4: Chromatographic overlay of six replicates of 5 ppb



Groundbreaking LC technology

The new Nexera LC-40 series merges ease-of-use and peace-of-mind



The Nexera series of UHPLC systems offers groundbreaking technology in terms of intelligence, efficiency and design, merging ease-of-use and peace-of-

mind. Advanced AI capabilities and lab management using the Internet of Things (IoT) have been integrated to monitor performance and resource allocation.

They make the new Nexera systems a leading-edge and user-friendly solution for versatile industries, setting new benchmarks in UHPLC.

Shimadzu has long been advancing the analytical performance of HPLC systems. The company has recognized that overall efficiency depends not only on the perform-

ance of one instrument, but on the management of all devices within a lab. That's where intelligence, efficiency and design come together.



The new Nexera systems are applicable to every analytical challenge with a seamless transfer between HPLC and UHPLC applications.

They stand for high reliability, extraordinary performance, exceptional reproducibility, ultra-low carryover and superior data quality. The instruments satisfy the needs of a wide range of applications for pharmaceutical, chemical, environmental, food, automotive and also clinical analyses.

A new benchmark of intelligence – maximizing reliability and uptime

The Nexera series provides auto-diagnostics functions as well as auto-recovery features supporting users in their day-to-day workflow. For example, air bubbles can in rare cases form in the mobile phase and cause problems if inhaled into the pump. Nexera has the ability to monitor baseline changes and pressure fluctuations to check for anomalies and take appropriate counter measures.

The Nexera UHPLC series maximizes reliability and uptime with fully unattended workflows that span from startup to shut-down. Operators can set the Nexera to start up at a specified time, so that it can complete auto-purge, equilibration, baseline checks and system suitability in advance, and be ready for analysis before they arrive at the lab. In addition, the smart flow pilot ramps up the flow rate gradually, reducing the possibility of damage to columns. There is no need to create startup protocols for each analysis.

Mobile phase levels can now be measured in real-time. Reservoir tray weight sensors monitor the volume of mobile phase or auto-sampler rinse solution in up to twelve containers, and can be checked remotely from a smart device. There is no need to worry about running out of mobile phase mid-analysis, as the system ensures beforehand that the vol-

ume will be sufficient for the entire run-time, otherwise giving a notification.

A new benchmark in efficiency – automating workflow, maximizing throughput

Automated processes and fast, robust performance are key to an efficient laboratory environment. They speed up the overall workflow and provide results even more accurate and reliable than before.

The Nexera series provides non-stop temperature-controlled analysis of thousands of samples with the new optional plate-changers. Samples can be set in advance in up to 44 MTPs or vial racks in each plate changer. Even during analysis, the insertion of additional vials and MTPs is possible due to the autosampler's

excellent temperature control.

A new benchmark of design – ease-of-operation with a reduced footprint

The set-up of the Nexera series merges

user-friendly functions with operational efficiency while space and cost-saving aspects provide a sustainable profitable solution for any laboratory.

The Nexera LC reduces energy consumption by over 80 % when on standby, significantly minimizing running costs and supporting an environment-friendly lab. Injection ports for two separate flow paths can be installed, allowing two different types of analysis to be performed at the same time using only one system. Nexera boasts ultralow carryover, even on a high-sensitivity LC-MS/MS. This reduces time spent on rinsing, resulting in a shorter overall analysis time.

Key components of the Nexera UHPLC series supporting laboratory efficiency:

- Mobile Phase Monitor MPM-40
- System Controller SCL-40, CBM-40
- Absorbance detector SPD-40 / SPD-40V and Photodiode detector SPD-M40
- Solvent delivery unit LC-40 series
- Autosampler SIL-40 series / Plate Changer
- Column oven CTO-40 series

The new Nexera series systems feature a uniquely small footprint and free up bench space for other instruments.

AI and IoT: ease-of-use meets peace-of-mind

Building on 40 years of experience in LC technology, Shimadzu has integrated groundbreaking technologies in the new Nexera LC-40 UHPLC series. AI (Artificial Intelligence) capabilities have been incorporated to allow devices to detect and resolve issues automatically. Lab management has been integrated using the Internet of Things (IoT) and device networking, making it simple to review the status of your instruments and optimize resource allocation.

Due to the combination of AI and IoT, the Nexera series foresees errors and helps to avoid common mistakes in order to guarantee the best possible outcome and efficiency. Smart software features allow close monitoring of instrument use while setting informed maintenance intervals. Users benefit from minimized downtime and maximized time-saving.



Everything styrene?

Material testing and infrared spectroscopic identification of plastics in recycling

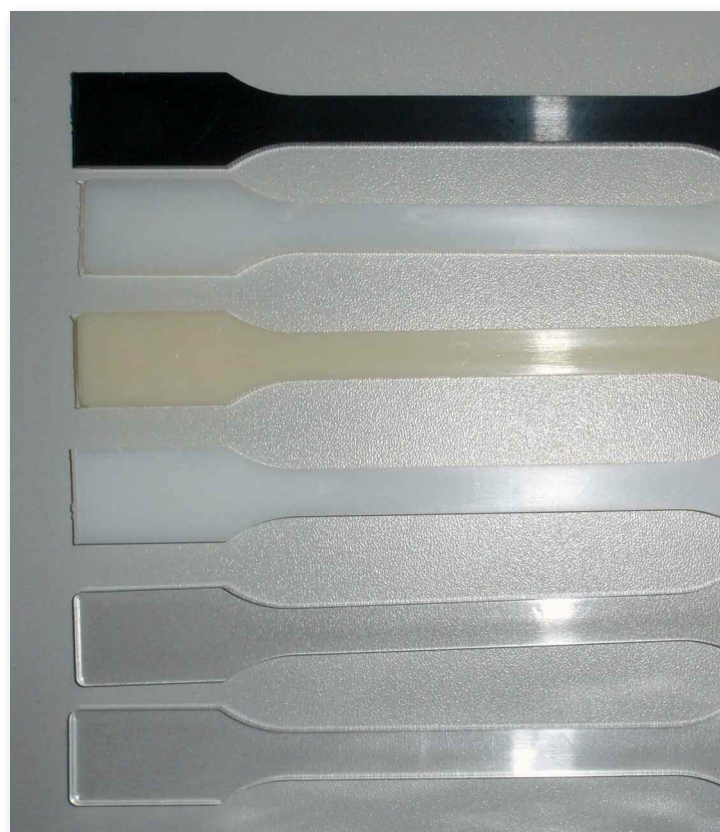
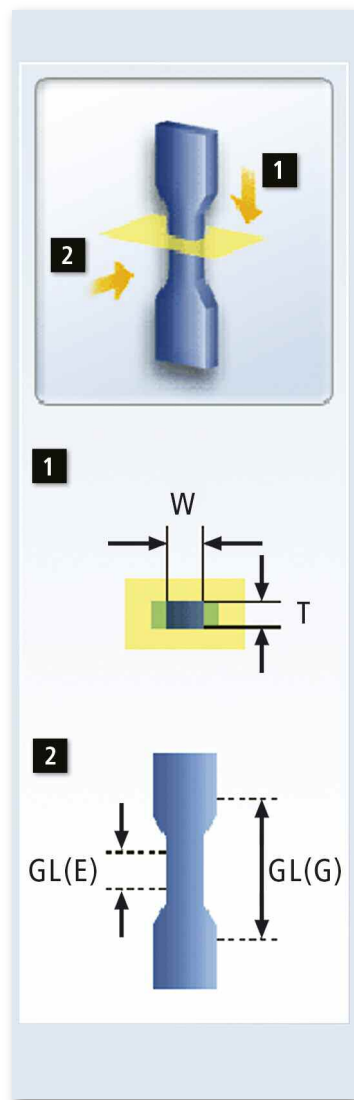


Figure 1: A test specimen in the sketch on the left, as deposited and clamped in the Trapezium software for ISO-527-1/2, where W (width) and T (thickness), GL (G) distance of the clamping tools and GL (E) are the distance of the markers for the video extensometer.

Real samples on the right (photo from bottom to top: GPPS (transparent), SAN (transparent), HIPS (milky), ABS (yellowish), ABS Magnum (milky) and ABS recycle (black) with dimensions $W = 10$ mm, $T = 4$ mm, $GL (E) = 50$ mm and $GL (G) = 115$ mm)

Plastic recycling is becoming ever more important – especially considering that mineral oil as a source of polymer raw material will not be available in this volume in the long run. The resources of the Earth and its atmosphere are finite. Among other things, „fresh“ polymer is produced from naturally occurring mineral oil. Depending on the intended use, different additives are added to support its product life. And at its end, the plastic ends up in the waste cycle. Under ideal conditions, the polymer is recycled and converted into

new forms with new properties, such as when a plastic with UV stabilizer and a plastic with plasticizers meet. After the recycling process, both polymers are fused and show new characteristics.

A complex task for recycling companies is to analyze and identify plastic waste and determine its mechanical properties. Based on these results, the plastic is separated into different categories in order to be able to further process it in a targeted manner. The mechanical properties of the plastic are important for the end

product. The specification for examination is based on ISO 527-1/2 [1]. By way of example, the challenges of polystyrene are considered in this article. This plastic group belongs to the family of styrene polymers.

Analysis of polystyrene

In this refining, polystyrene is considered as GPPS (General Purpose Polystyrene). As a homopolymer, it is very brittle. To reduce the brittleness, small amounts of BR (butyl rubber) can be added, resulting in an impact-

resistant GPPS: HIPS (High Impact Polystyrene). The disadvantage of both is the low chemical temperature resistance.

This property can be improved by adding acrylonitrile to GPPS. The result is SAN, a styrene-acrylonitrile copolymer. Acrylonitrile influences the strength, toughness and durability of polystyrene. In addition, butadiene can be added to improve the properties of SAN resulting in ABS (acrylonitrile-butadiene-styrene copolymer). ABS is considered to be impact-resistant when compared to the precursors.

In the recycling sector, there are already plastics with corresponding additives and co-polymers in bulk. For further processing, it is important to know what can be improved in terms of content in order to achieve the desired properties.

Samples for testing according to ISO 527-1/2:

Test specimens were produced by injection molding. The bodies are shown in figure 1. On the left, sketches show the test positions in the clamping tool and on the right, the real samples can be seen.

Identification

Infrared spectroscopy can be used to identify the polymer by rapid screening. Measurement takes place within seconds with the help of ATR spectroscopy. For this purpose, an IRSpirit-T FTIR instrument was used, equipped with the integrated QATR-S and accessory detection.

The specimen is clamped in the ATR with reproducible pressure. Infrared radiation can penetrate into the sample surface according to the rules of attenuated total reflection. This reacts to the IR

heat with vibrations that are characteristic of the polymers.

Identification of the polymer is supported by the LabSolutionsIR software in combination with libraries. Since the styrene polymers have related spectra, attention must be paid to specific vibrations in the infrared spectrum, which differentiate these possible mixed variants.

Different variants of polystyrene have been investigated. In order to test the quality of the surface of a sample (figure 1), they were tested with a 10-fold determination. Five measuring points were measured in each case on the two flat sides of the test piece.

With this in mind, ABS blends were analyzed – an ABS recycle and an ABS with BX declared sample. According to the infrared spectrum (figure 3, page 16), the ABS recycle is a mixture

Abbreviation	Description	Chemical structure	Comment
SAN	Styrene-acrylonitrile		Contains ~20 % ACN
ABS	Acrylonitrile-butadiene-styrene		Contains ~20 - 25 % ACN, ~15 - 30 % butadiene
ACN	Acrylonitrile		
GPPS	General purpose polystyrene		Crystal clear, without additives
HIPS	High impact polystyrene		Shock resistant, contains 4 - 12 % BR, thermoplastic
BR	Butadiene rubber (rubber)		One variation of BR, cis-1,4-polybutadiene is shown here
PC	Polycarbonate		PC is ~40 - 70 % included in ABS and becomes PC-ABS
PPG	Polypropylene glycol		Additive

Table 1: Explanation of the plastic abbreviations, structural chemical formula and properties of the styrenes considered

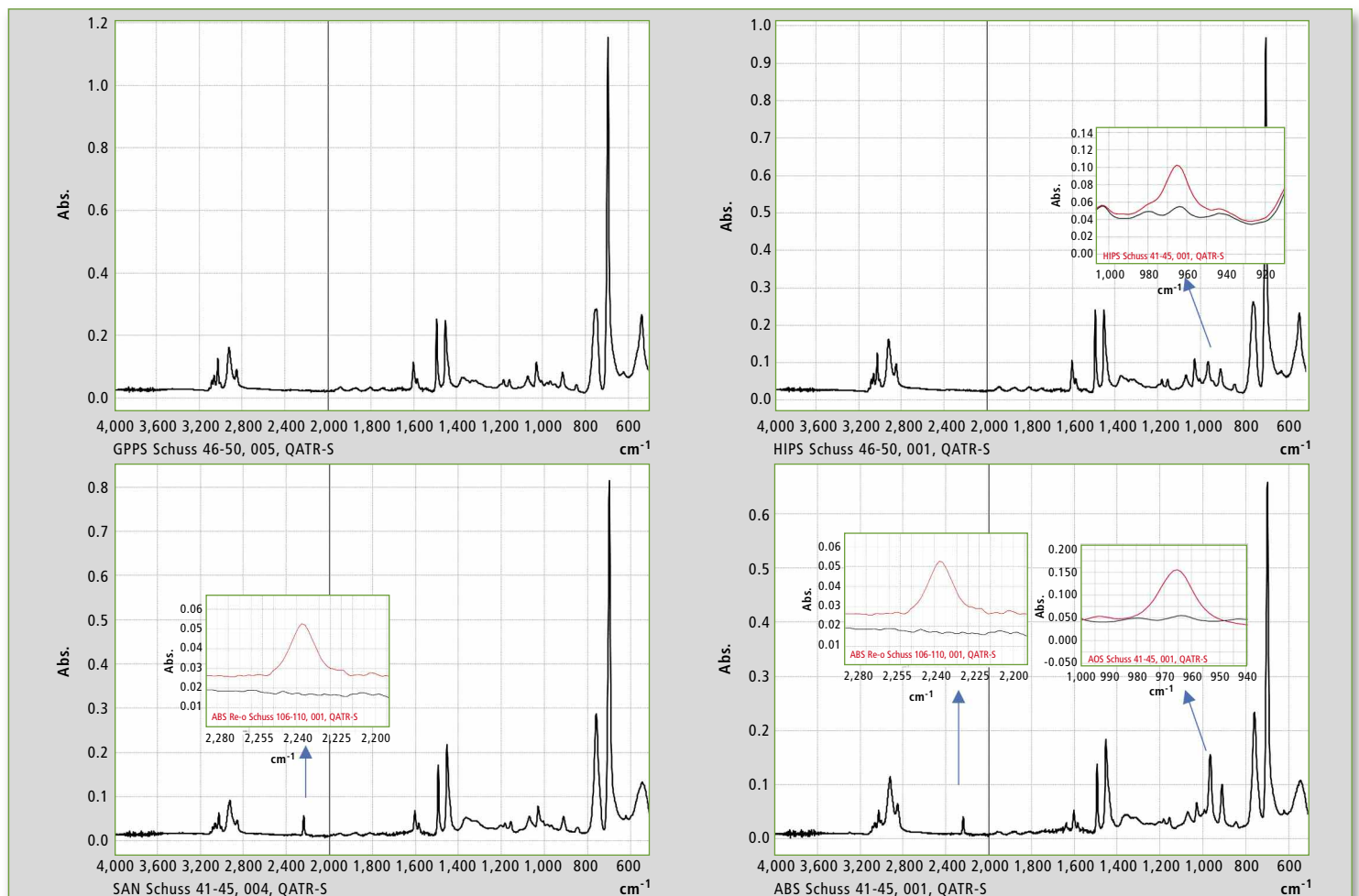


Figure 2: Infrared spectra of the examined polystyrenes and comparison to the GPPS spectrum, top right HIPS with 965 cm^{-1} by BR-shares, bottom left SAN with the nitrile-part at 2,237 cm^{-1} and bottom right the target to produce an ABS: here in the polystyrene spectrum at 2,237 cm^{-1} the nitrile signal is visible and at 965 cm^{-1} the signal of butadiene is visible.

of ABS with a high content of styrene, PC and methacrylate. By contrast, the ABS with the BX logo represents a mixture of ABS with a high content of styrene and polypropylene glycol (PPG, plasticizer). With the help of a library search and subtraction spectroscopy, the different components could be found in the mixtures.



Universal testing machine AG-Xplus

To assess the quality of the mixtures, the nitrile and styrene/butadiene bands in the IR spectra were

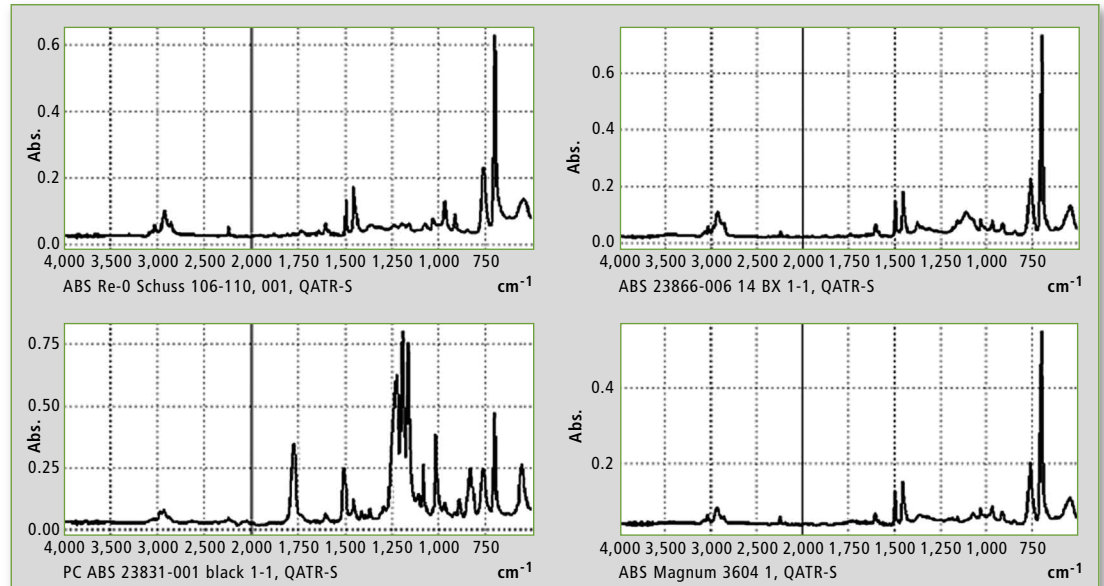


Figure 3: Infrared spectra of four samples, which contain not only the polymers of table 2. On the bottom right is an ABS, bottom left is the mixture of PC and ABS, top left is a recycled material with ABS and parts of PC (structure around 1,240 cm^{-1}) and on top right is an ABS with parts of PPG (1,110 cm^{-1}).

Polymer	Analytical wave-number (cm^{-1})	Molecular group
GPPS	no 2,237, low 965	Pure styrene
HIPS	965; 1,451.5	Butadiene
SAN	2,237	Nitrile
ABS	2,237; 965	Nitrile and butadiene

Table 2: Differentiation of the styrene polymers based on IR vibrations

selected for analysis. In each case, 50 measurements (five test pieces with ten measurements each) were evaluated. Standard deviation of the results showed the maximum of the signal positions to be 0.00x absorbance units. This is excellent quality for the test specimens on the surface (table 3).

Mechanical test according to ISO 527-1/2 with the AG-Xplus universal testing machine

Infrared spectroscopy was used to investigate the surface of the samples with regard to identification of the plastics and testing of the homogeneity at the surface.

A layer thickness of approximately 4 μm of the 4 mm thick specimens was detected from the outside. To assess homogeneity with respect to the whole layer thickness, a mechanical test can complement the FTIR measurement results. To compare the samples, the elasticity of the polymers according to ISO 527-1/2 was evaluated.

Elasticity was measured using a non-contact extensometer with a TRViewX Video Extensometer. It can determine the yield strength with high accuracy. With the accompanying TRAPEZIUM

Sample	Average nitrile [Abs.]	Standard deviation [Abs.]	Variance [%]	Average styrene/butadiene [Abs.]	Standard deviation [Abs.]	Variance [%]
ABS + BX (1)	0.22698	0.00209091	2.44E-09	0.23032	0.00328504	7.68E-09
ABS + BX (2)	0.17364	0.00656943	3.40E-08	0.17755	0.00436416	1.22E-08
ABS Magnum (1)	0.28266	0.00310196	2.00E-08	0.25458	0.00415743	7.35E-08
ABS Magnum (2)	0.30668	0.00669716	4.00E-07	0.27317	0.00569431	2.15E-07
ABS + PC	0.32116	0.00525913	4.81E-08	0.41128	0.00315633	4.33E-09
ABS Re-0 (2)	0.26404	0.00954735	2.30E-07	0.36145	0.00562222	7.22E-08
ABS Re-0 (2)	0.26514	0.00644689	8.46E-08	0.36067	0.00494152	6.51E-08
ABS (1)	0.23802	0.01156123	5.02E-07	0.42917	0.0045808	3.04E-08
ABS (2)	0.23408	0.00751945	1.33E-07	0.43198	0.0035035	4.39E-08
GPPS (1)	0.13538	0.01630428	3.19E-06	0.13445	0.02193037	9.42E-06
GPPS (2)	0.11752	0.00346821	5.68E-08	0.12503	0.01270058	1.61E-06
HIPS (1)	0.10386	0.00227902	3.08E-09	0.21248	0.00279107	5.11E-09
HIPS (2)	0.10886	0.00230573	7.18E-09	0.21467	0.00471224	2.65E-08
SAN (1)	0.26648	0.00430523	2.09E-08	0.08418	0.00348568	1.52E-08
SAN (2)	0.26286	0.00159453	1.70E-09	0.08357	0.00220972	4.35E-09

Table 3: Quality Control by FTIR at selected analytical wavelengths for determining the height of the nitrile signal (2,230 cm^{-1}) and styrene/butadiene signal (965 cm^{-1}), mean value of 50 measurements per test lot of five specimens including standard deviation and variance

software, the measurement conditions and video monitoring can be set up.

The sample was clamped with a preload of five N. For video surveillance, the test specimens were provided with markers which were placed at a distance of 5 cm. By using the video camera, the test area was detected and the middle part of the test specimen was set up in the digitally specified marking.

The ISO prescribes at least five test pieces, which were measured accordingly in this test series. The polymers with „soft“ characteristics were tested with a tension of 20 mm/min, while the „brittle“ specimens (GPPS, HIPS) were tested at 2 mm/min.

Figure 4 shows the typical curves of Newton's force versus „Millimeter distance“ for the five lot samples. Except for one partial sample, all test specimens showed good reproducibility. Results of the other lots were reproducible. The ABS Magnum lots showed greater deviations in the elasticity measurements while the force-

Plastic	E-Module (Mpa)	Tensile strength/stretch stress (MPa)	Ultimate elongation/stretching elongation (%)
SAN (d = 1.08)	3,600 - 3,900	70 - 85	5
ABS (d = 1.04 - 1.06)	1,300 - 2,700 (220 - 3,000)	32 - 45	15 - 30
PS (d = 1.05)	3,200 - 3,250	45 - 65	—
GPPS	—	—	—
HIPS (d = 1.04 - 1.08)	—	42	—
PC (d = 1.20)	2,100 - 2,400	56 - 67	100 - 130
ABS + PC (d = 1.08 - 1.17)	2,000 - 2,600	40 - 60	—

Table 4: Properties [2] of selected plastics after the plastics test ISO 527-1/2

Plastic	E-Module (Mpa)	Max. force (N)	Yield stress (MPa)	Stretching elongation (%) based on extensometer
ABS Re-0 (1)	2,202.97	1,533.3	40.12	2.47
ABS Re-0 (2)	2,342.89	1,515.77	40.46	2.1
ABS (1)	2,108.68	1,621.78	42.43	2.61
ABS (2)	2,095.31	1,630.28	42.66	2.65
ABS+PC	2,219.21	1,903.5	49.8	3.78
ABS + BX (1)	2,918.66	1,826.29	47.78	1.42
ABS + BX (2)	2,464.77	1,841.14	48.17	2.52
HIPS (1)	1,328.97	868.12	22.71	62.34
HIPS (2)	1,391.93	864.74	22.62	61.96
GPPS (1)	—	1,359.59	35.57	—
GPPS (2)	—	1,337.93	35.01	—
SAN (1)	—	2,672	69.92	—
SAN (2)	—	2,550.41	66.73	—
ABS Magnum (1)	2,239.22	1,517.5	39.7	2.4
ABS Magnum (2)	1,603.43	1,506.95	39.43	5.69

Table 5: Results of measurements with AG-XPlus in combination with TRViewX according to ISO-527-1/2 for the plastic samples (average of five test specimens of one lot)

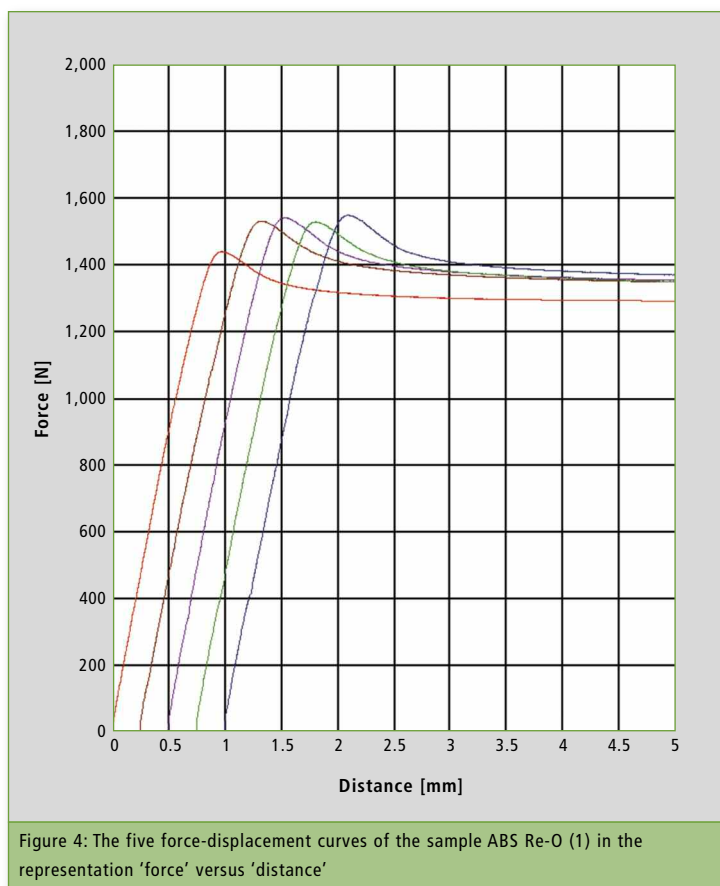


Figure 4: The five force-displacement curves of the sample ABS Re-O (1) in the representation 'force' versus 'distance'

displacement curves were reproducible (figure 4).

Conclusion

With non-destructive infrared spectroscopy, polymers in the form of test specimens (as per ISO 527-1/2) can be identified and tested for homogeneity on the surface. Standard deviations in the order of magnitude of less than 0.01 ABS units at selected signal positions are due to the noise of the equipment and accessory combination and indicate a good reproducibility of the test specimens.

This was confirmed for the complete layer thickness by tensile testing (ISO-527-1/2) of the materials. For the plastics recycling industry, this analysis is indispensable for determining properties of the plastic polymers of the styrene family.

Acknowledgments

Many thanks to Carat GmbH (Bocholt, Germany) for advice on the subject and provision of the plastic samples. The application was developed in collaboration with Erwin Jansen and Albert van Oyen (both Carat GmbH).

Literature

- [1] „Plastics – Determination of tensile properties“, DIN EN ISO 527-1/2
- [2] „Saechtling Kunststoff Taschenbuch“, 31. Auflage, Hanser Verlag, 2013



Safety first – well protected with guard columns

Guard columns in chromatography protect the analytical separation column. Will they affect the separation?

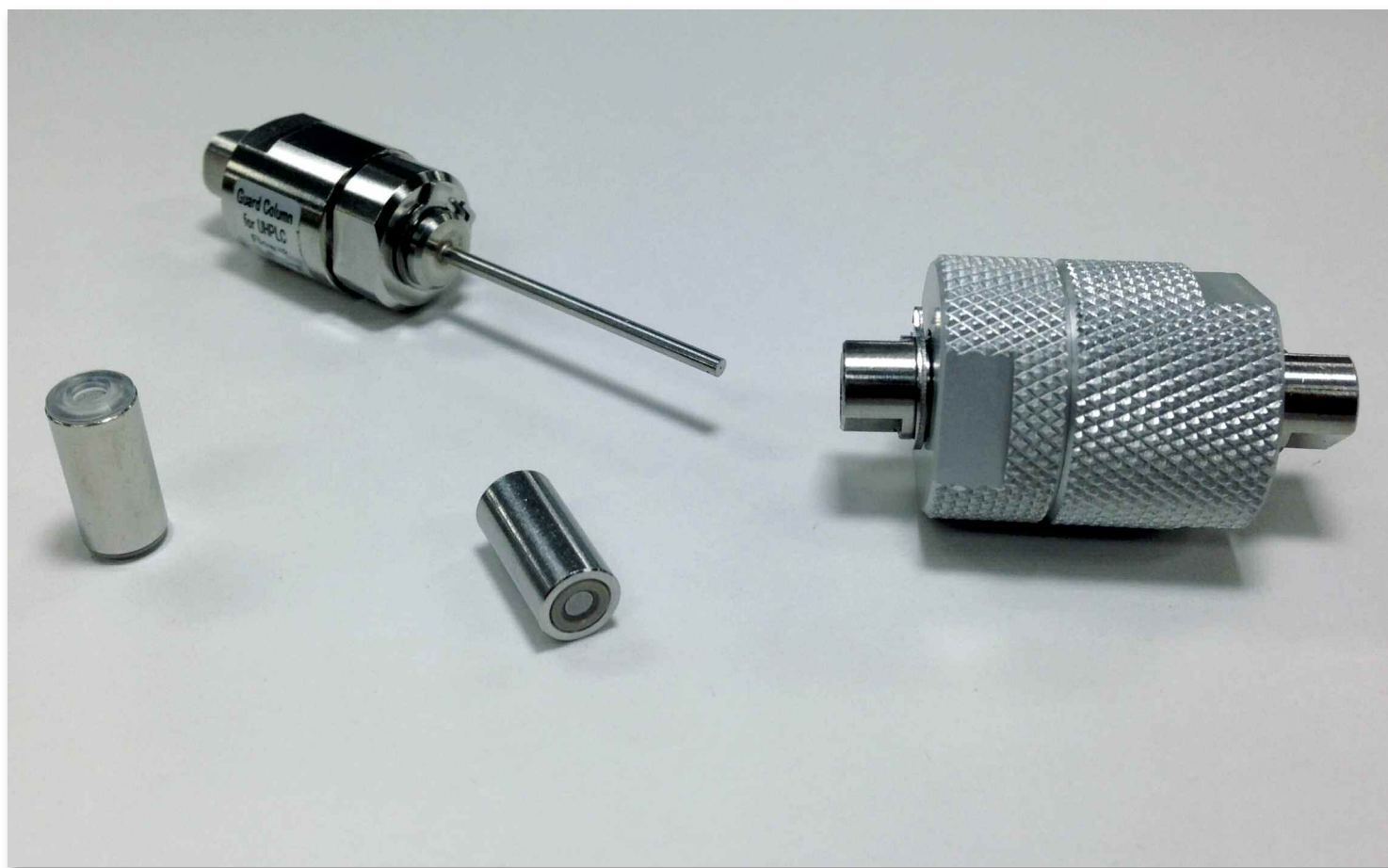


Figure 1: G-series holder (high pressure and conventional type) with cartridges

Guard columns are familiar to anyone working in chromatography, but they are by no means used in every analysis. This article explains guard columns and their function as well as the advantages and disadvantages.

A guard column is a typical consumable. It is installed in front of the main column and protects it from impurities that can come from the sample, matrix or eluent by collecting and trapping particles and/or irreversibly binding

substances. It extends the lifecycle of the more expensive main column and, being the cheaper component, is replaced more often.

Function of a guard column

The guard column is smaller than the main column and is usually equipped with the same packing material. In the best case, particle sizes of the guard and main columns are identical. The inner diameter of the column and the size of the frit should be equal or smaller, and the pressure specifica-

tions of the guard column should match those of the main column.

Anyone who has ever changed the filter at the top of the column is aware of the impurities that often accumulate there. Contaminations may originate from the sample or

sample matrix. The guard column traps them in front of the main column with various protective measures: [1]

1. Chemical protection: If the matrix or sample are particularly aggressive, they may react

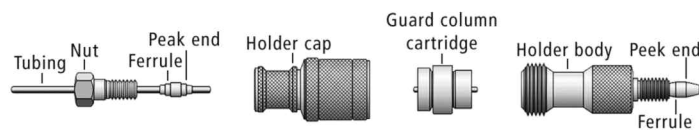


Figure 2: Schematic structure of the Velox guard column

with the column material. In this case, provided the guard column is made of the same material as the separation column, most substances react with the guard column and the analytical column is protected.

2. Particle trap: If the guard column has the same porosity as the analytical column, any particles larger than the frit are trapped by the guard column before they reach the analytical column where they get caught and block it.

3. Other polarities: Analytes with different polarities can adhere to the packing material of the guard column and interact so strongly that they remain irreversibly bound to the stationary phase (of the guard column) and accumulate.

So-called in-line filters trap larger molecules and are the cheapest option to protect the separation column [1]. However, they only work physically and not chemically. The filling material is a filter with a specific porosity. Compared with the column, it should be slightly smaller so that the inline filter captures particles before they enter the column. As soon as system pressure starts to rise, it's time to swap the inline filter, as the increase in pressure indicates that the filter is blocked with particles. Compared to the guard column, its replacement is quicker, as is the subsequent system conditioning.



Figure 3: Velox guard column

Column type	Guard column type
G-series	G-series
XR-series	No special guard column available; G-series recommended
VP-ODS	VP-ODS
Velox Core Shell series	Velox Core Shell series

Table 1: Column types in the Shim-pack assortment with corresponding guard column type

Influence of a guard column on the separation

When adding a guard column, an increase in the plate number N would be expected, because with the additional guard column, the system, contains more stationary phase. However, this effect is mostly lost by the fact that more dead volume is created in the system when installing a guard column. If the capillaries used to connect the guard column are too long, this effect may even adversely affect the chromatogram. [2]

A guard column behaves like an extra piece of separation column, so when in use, it always increases the system pressure.

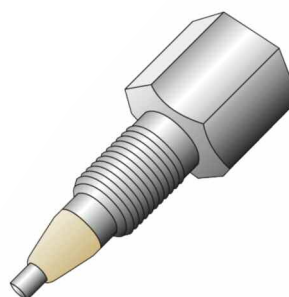


Figure 4: Velox precolumn filter

For these reasons, it should be as short as possible (often 1 - 5 cm, typically 0.5 - 2 cm) to avoid increase in system pressure and to minimally influence the chromatographic separation. [1] The effects of guard columns on chromatographic separation are examined below by assessing different column types with and without the associated guard column.

Changing the guard column

Many users are unsure of when a guard column should be replaced. There are several indications of the need for change. When the system pressure increases, this is a sign that particles have accumulated and are slowly clogging it.

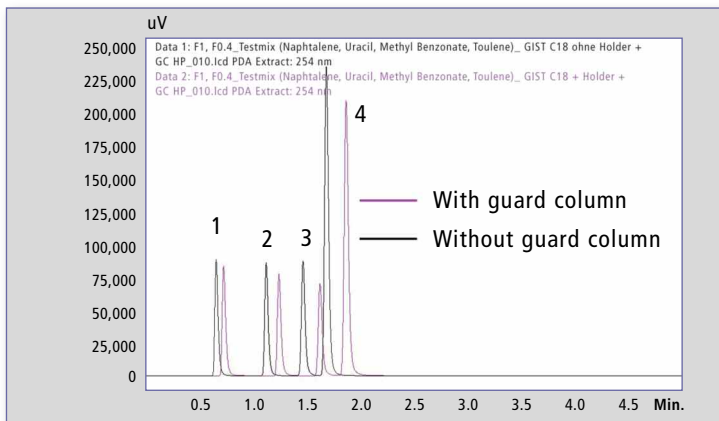


Figure 5: Chromatogram with and without guard column G-series (conventional). Peak 1: uracil, peak 2: methyl benzoate, peak 3: toluene, peak 4: naphthalene

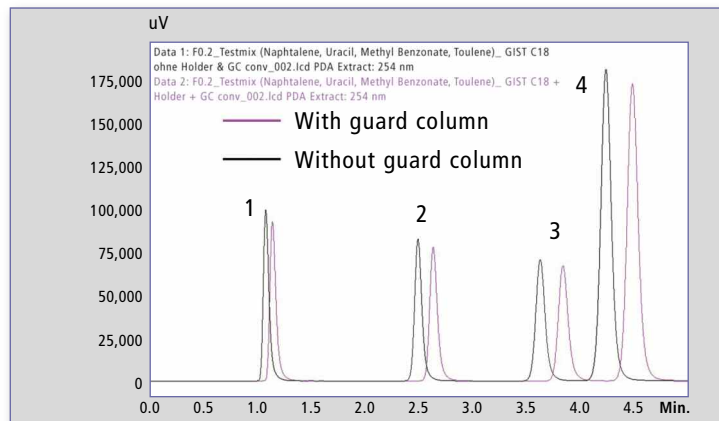


Figure 6: Chromatogram with and without G-series guard column (high-pressure type). Peak 1: uracil, peak 2: methyl benzoate, peak 3: toluene, peak 4: naphthalene

	N	t _R [min]	k	Height [µV]	Area [au]	Width 0.5 [min]	Pressure [bar]
With guard column	9020	4.48	2.90	172232	1262248	0.111	63
Without guard column	8989	4.24	2.90	180937	1256453	0.105	55
Change with guard column	+0.3 %	+5.5 %	±0 %	-5.1 %	+0.5 %	+5.4 %	+12.7 %

Table 2: Results of naphthalene on the conventional column of the G-series with corresponding guard column

	N	t _R [min]	k	Height [µV]	Area [au]	Width 0.5 [min]	Pressure [bar]
With guard column	10680	1.87	1.56	205972	586538	0.043	304
Without guard column	9676	1.69	1.55	232758	625486	0.040	272
Change with guard column	+9.4 %	+9.7 %	+0.7 %	-13.0 %	-6.6 %	+6.9 %	+10.5 %

Table 3: Results of naphthalene on the high-pressure column of the G-series with corresponding guard column

Another indication may be a decreasing number of plates or a change in the signal. Alternatively, the user may specify a certain maximum number of injections. As a rule of thumb, the guard column is changed approximately three times during the service life of the main column.

Types of guard columns

There are different types of guard columns:

- **packed guard columns** – these are simply „mini-variants“ of the analytical columns
- **the „cartridge type“** – here, small cartridges are placed in a holder and can be installed in front of the column.

Shimadzu’s Shim-pack range includes both types; they are explained in the following section.

Guard column types in the Shim-pack portfolio

The LC Column range offers a choice of different types of guard

columns to fit different LC columns. The most important series with the associated guard columns are shown in table 1 (page 19).

The guard column holders and cartridges of the Shim-pack G-series (figure 1, page 18) are available as a high-pressure version (holder in the top of the picture) and in a conventional version (holder in the bottom of the picture). The former is pressure stable up to 800 bar, whereas the conventional version is compatible for analyzes up to 200 bar. The high-pressure guard column can be installed with an additional fitting. For the conventional guard column, a short capillary with two fittings is needed as a connecting piece.

The Velox core shell series guard columns are used in the same way. The guard column cartridge is mounted in a holder and then installed in front of the column. The schematic principle is shown in figure 2 (page 18) and the assembled guard column is shown in figure 3 (page 19). This guard

column can be installed directly in the system without additional fittings. In addition, a built-in spring provides safe installation with minimal dead volume.

With the introduction of the Shim-pack Velox columns in autumn 2018, the Shim-pack Velox UHPLC precolumn filters have also been added to the range (figure 4, page 19). They do not contain a stationary phase but a porous material (0.2 µm), so they act purely physically and trap too

large particles before they reach the main column. The guard column filter replaces or supports sample preparation with syringe filters.

The ideal guard column would in no way affect chromatographic separation and would not change the system pressure. The next part of the experiment investigates how the various Shim-pack guard columns affect the chromatograms.

Measurement parameters and methods

Instruments: LC-2040C 3D (Shimadzu)

Column: Shim-pack GISS C18-HP (100 mm x 2.1 mm I.D., 1.9 µm); **Guard column:** Shim-pack GISS C18-HP (10 mm x 2.1 mm I.D., 1.9 µm)

Column: Shim-pack GIST C18 (100 mm x 2.1 mm I.D., 3.0 µm); **Guard column:** Shim-pack GIST C18 (10 mm x 1.5 mm I.D., 3.0 µm)

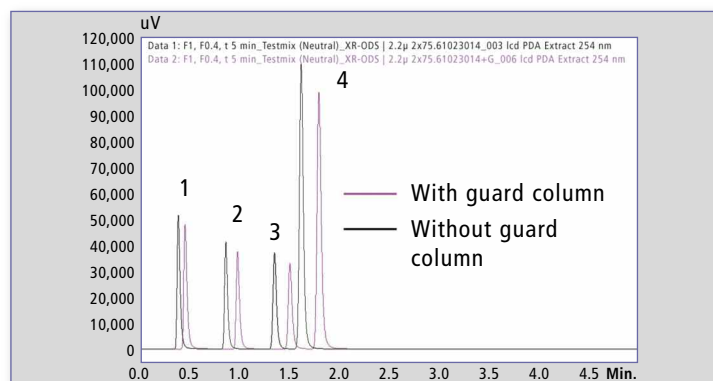


Figure 7: Chromatogram XR ODS II with and without G-series guard column (high-pressure type). Peak 1: uracil, peak 2: methyl benzoate, peak 3: toluene, peak 4: naphthalene



Column: Shim-pack XR-ODS II (75 mm x 2.0 mm I.D., 2.2 µm);
Guard column: Shim-pack GISS C18-HP (10 mm x 2.1 mm I.D., 1.9 µm)

Column: Shim-pack Velox SP-C18 (100 mm x 2.1 mm I.D., 2.7 µm);
Guard column: Shim-pack Velox EXP SP-C18 (5 mm x 2.1 mm I.D., 2.7 µm)

Mobile Phase: 35 % H₂O;
 65 % ACN

Sample: Uracil (20 µg/mL), methyl benzoate (220 µg/mL), toluene (860 µg/mL), naphthalene (200 µg/mL), dissolved in the eluent

Oven temperature: 40 °C

Flow rate: 0.4 mL/min,

0.2 mL/min for the GIST C18 (100 mm x 2.1 mm I.D., 3.0 µm);

Injection volume: 0.5 und 1.0 µL

Results

In the following results and values of the chromatogram, the last eluting peak (naphthalene) is always taken as a comparison since the influence of changes is greatest here. The chromatograms show that guard columns have a slight influence on measurement results. If guard and main columns match, overall measurement results will be less affected than when using guard columns with main columns of a different type.

Columns and guard columns of the Shim-pack G-series

Tables 2 and 3 and figures 5 and 6 (page 19) show the examination of columns and guard columns of the Shim-pack G-series (conventional and high pressure type). In figures 5 and 6, it becomes clear that the use of a guard column results in more retention, i.e. a longer retention time. This can be explained by the additional stationary phase in the form of the guard column. This effect occurs with each use of a guard column, as the separation distance as well as the volume in the system increase through it. If the guard column is connected to additional capillaries, more dead volume will be created in the system.

Along with longer retention time, signal intensity also decreases min-

	N	t _R [min]	k	Height [uV]	Area [au]	Width 0.5 [min]	Pressure [bar]
With guard column	72729	1.79	3.04	98205	305881	0.046	215
Without guard column	6713	1.62	3.30	110222	313313	0.042	187
Change with guard column	+7.8 %	+9.9 %	-8.8 %	-12.2 %	-2.4 %	+8.7 %	+13.0 %

Table 4: Naphthalene results from the XR-ODS II Column with matched guard column from the G-series

	N	t _R [min]	k	Height [uV]	Area [au]	Width 0.5 [min]	Pressure [bar]
With guard column	8806	1.45	1.66	123473	308226	0.036	149
Without guard column	8222	1.38	1.66	119029	291206	0.036	134
Change with guard column	+6.6 %	+7.8 %	±0 %	+3.6 %	+4.5 %	±0 %	+10.1 %

Table 5: Naphthalene results on Velox Core Shell column with corresponding guard column

imally. Measurement values are shown in tables 2 and 3. As expected, the plate number N increases with retention time. This effect is also based on the additional separation performance of the guard column. As a result, the width of the signals also increases slightly. The pressure in the system increases by 12.7 % (conventional type) and 10.5 % (high pressure type) in the columns.

Since the guard column was chosen in the same dimensions as the main column, an additional, narrow separation phase in the system increases the pressure. The retention factor shows no or only slight deviations. This is a very positive effect and shows that the guard column fits very well with the main column.

XR-ODS II columns without matching guard column

In a separate step, XR-ODS II columns were studied with a modified G-series guard column since there are no XR-ODS guard columns available.

Results in figure 7 and in table 4 are similar to those of the G-series. The guard column, retention time, plate number, signal width and pressure increase, whereas the height and area of the signals decrease. As a negative effect, it can be seen that the retention factor k decreases by almost 9 %. Ideally, this would hardly change. Here, it is clear that the guard column does not fit the main column.

Velox core shell columns with and without guard column

Results of Velox core shell columns with and without guard columns are shown in figure 8 and table 5. Here, the best results are compared to the other columns. Retention time and the number of plates increase, but so do signal heights and area when using a guard column. Peak width and retention factor do not change. Also with

Conclusion

A guard column protects the expensive analytical column by capturing contaminants or particles. It may be replaced regularly, thereby increasing the life of the analytical column. The use of guard columns makes sense if the sample, matrix or eluent contain impurities or substances that react with or clog the column material. The investigations have shown that analytical separation is only

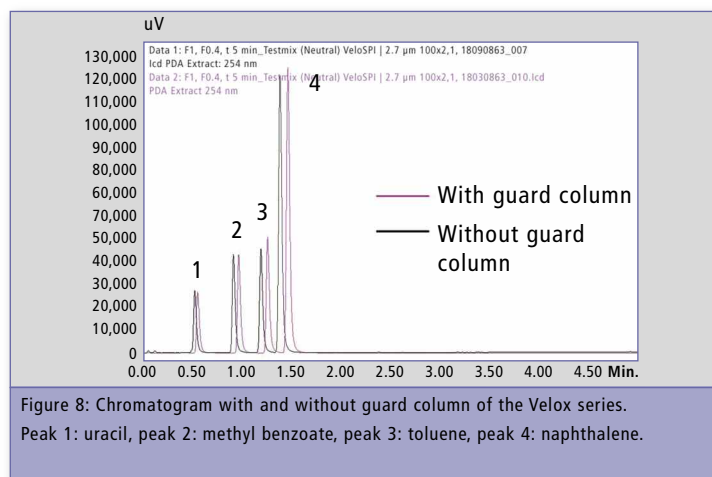


Figure 8: Chromatogram with and without guard column of the Velox series. Peak 1: uracil, peak 2: methyl benzoate, peak 3: toluene, peak 4: naphthalene.

the Velox column, system pressure increased by 10 % when using the guard column.

Overall, the results show that guard columns have little effect on analytical measurement and may even change many parameters in a positive sense. The system pressure should always be well monitored when using a guard column.

minimally influenced by the use of a guard column. The user can therefore (apart from very critical separations) safely apply a guard column to increase the life span of the analytical column and thereby save costs.

Literature

- [1] J.W. Dolan, LCGC, Volume 11, Issue 1.
- [2] J.W. Dolan, LCGC North America, Volume 32, Issue 12, 2014.



What a smell!

Identification of pyrazines and methional by heart-cut GC-O/GC-O/MS

The taste of potato chips or grilled vegetables has to do with pyrazines and methional, two chemical compounds responsible for a roasty flavor in food. Both are connected to the heat-initiated Maillard reaction of reducing sugars and amino acids, adding taste and smell to vegetables and meats.

The aim of these current investigations was to identify co-eluting potent odor-active compounds in a natural flavor extract. This was achieved by GC-O, a gas chro-

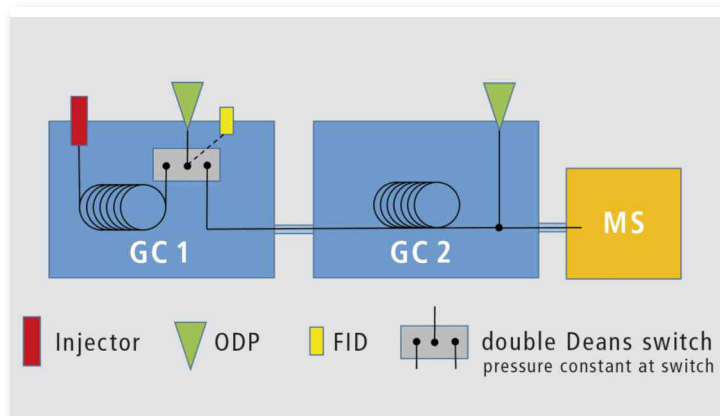
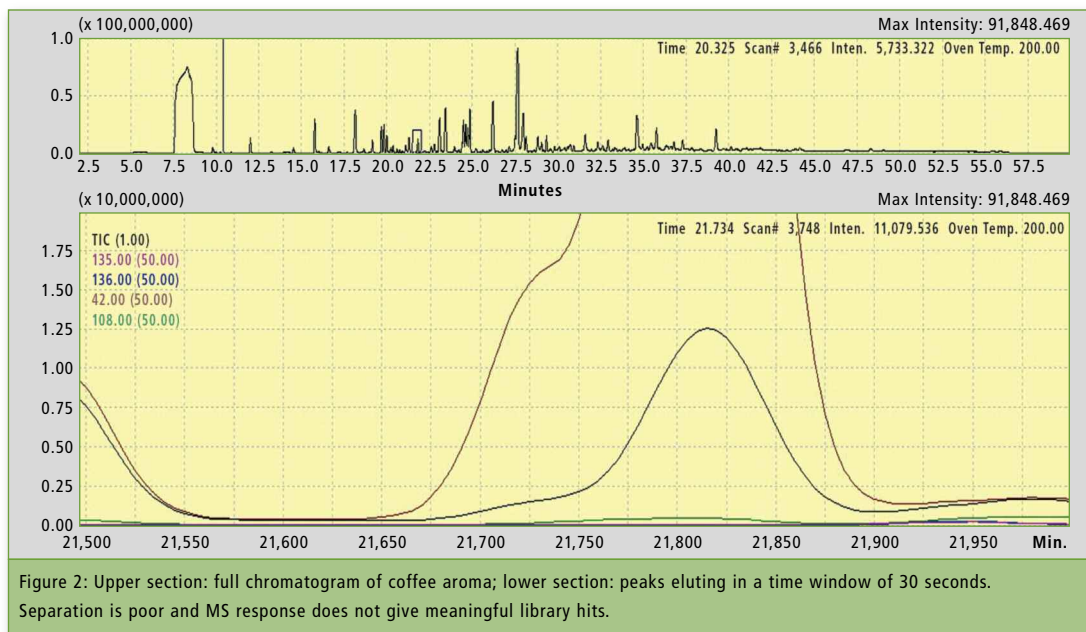


Figure 1: Instrumental set-up of the GC-O/GC-O/MS system

matographic olfactometric method in combination with two-dimensional GC-MS, gas chromatography and mass spectrometry. The GC-O method is the perfect choice for analysis of individual odor relevant substances in complex blends. It enables recognition of substances which other analytical methods are unable to identify due to lower detection limits.

A GC-O/GC-O/MS system (figure 1) was used to transfer this elution range from the first column (DB-FFAP) to a second col-



transferred to the second column and analyzed using MS. Figure 3 shows a very good separation of compound eluting in this time slot with perfect conditions for identification and GC-O analysis on the second sniffing port.

Materials and methods

GC-O/GC-O/MS was performed using a Shimadzu GC-2010 gas chromatograph connected to a Shimadzu GCMS-QP2020, a single quadrupole for monitoring of

microscopic quantities of functional compounds. In the first dimension the separation of the extract was achieved on an OPTIMA® FFAPplus column (length 30 m, diameter 0.25 mm, film thickness 0.5 μm). The chromatographic area of interest was transferred to a second capillary column OPTIMA 5 column (length 30 m, diameter 0.25 mm, film thickness 0.1 μm) by means of a Deans Switch.

Sniffing analysis was executed on FlavoLogic sniffing ports which

can be mounted and heated by an additional Shimadzu injector. These sniffing ports have an optimized geometry for most sensitive detection and no tailing of odors from re-condensing aroma compounds (figure 4, page 24). ♦

column (DB-5) by means of a heart-cut Deans Switch system. The compounds eluting from the second column were also evaluated by means of simultaneous GC-O and GC-MS. The DB-FFAP column is of high polarity and particularly suitable for the analysis of aroma compounds. The DB-5 is an almost non-polar phase and separates, what the FFAP cannot separate.

The principal strength of this strategy is best demonstrated on the example of a coffee extract. Figure 2 shows in the upper section a total chromatogram of a coffee extract and in the lower section compounds eluting in a narrow time window of 30 seconds. The peaks in this window are badly shaped and MS library searches fail. This area was now

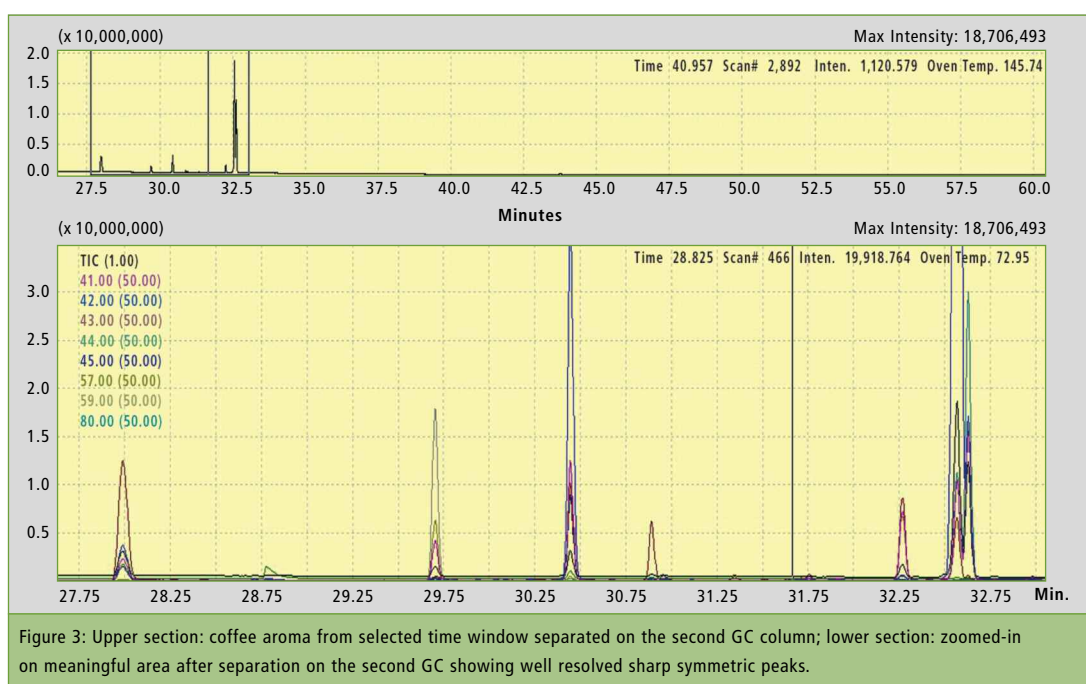




Figure 4: Sniffing at the FlavoLogic GC-O/GC-O/MS system

Experiment and results

A natural flavor extract separated on a DB-FFAP column showed interesting sniffing impressions in a small time window around 23.1 and 23.3 min (figure 5). The odors were perceived as roasted, earthy and cooked potato-like. Reference data revealed that methional and a couple of pyrazines as potential aroma compounds elute in this area. However, one-dimensional GC-MS data gave no reliable MS signals. Also, it was assumed that the peak in the area of interest is the result of a difficult co-elution situation, and that potentially more than one pyrazine is co-eluting with methional.

After transfer of these peaks into the second column, three closely eluting peaks were detected at a retention time range from 34.40 - 34.65 min on DB-5, all three of them exhibiting roasted, pyrazine-like odor notes when sniffed at the sniffing port (figure 6). Evaluation of mass spectra and comparison with reference compounds enabled the identification of peak 1 (34.45 min) as 3-ethyl-2,5-dimethylpyrazine, of peak 2 (34.52 min) as 2,6-diethylpyrazine and of peak 3 (34.60 min) as 2,5-diethylpyrazine.

In addition, a potato-like smelling peak was detected at 29.875 min and confirmed by MS to be methional (figure 7).

Summary

The results show that GC-O/GC-O/MS is a perfect method for identification of co-eluting potent

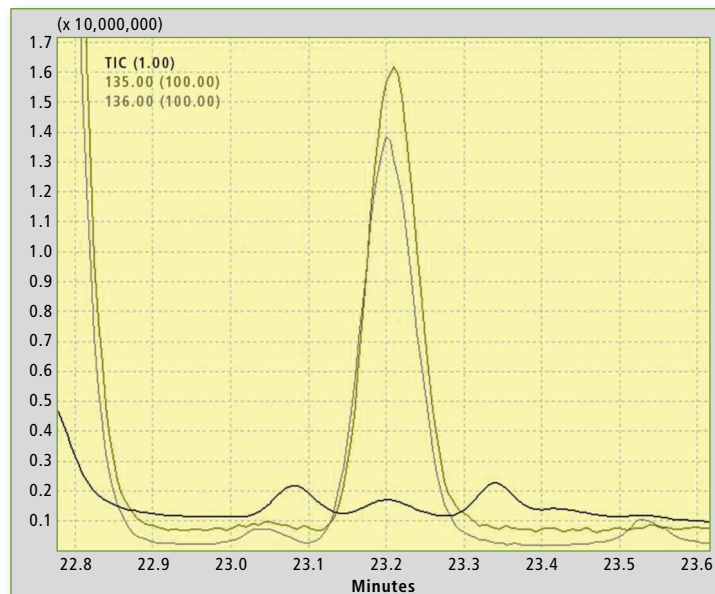


Figure 5: Asymmetrical shaped peak after separation on the first column

odor-active compounds in natural flavor extracts due to their very good separation. With a heart-cut Deans Switch system, evaluation of the mass spectra and compari-

son with reference compounds enabled precise identification of definite chemical compounds.

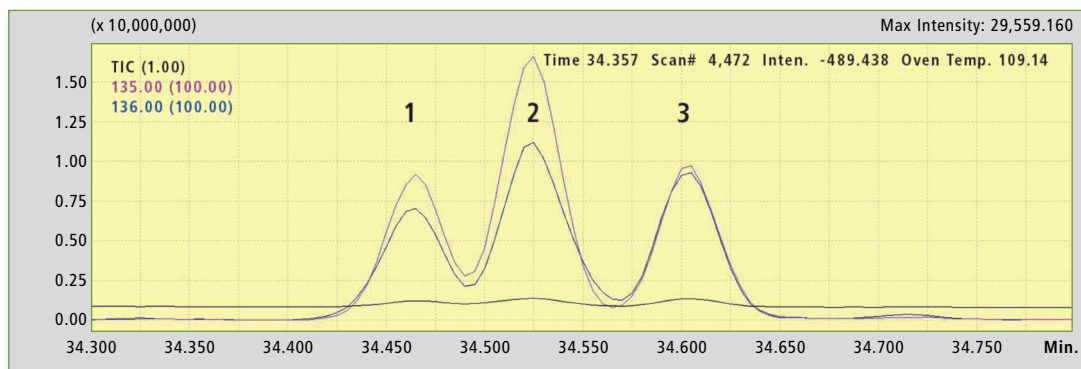


Figure 6: Three pyrazine peaks after heart-cut and separation on second column

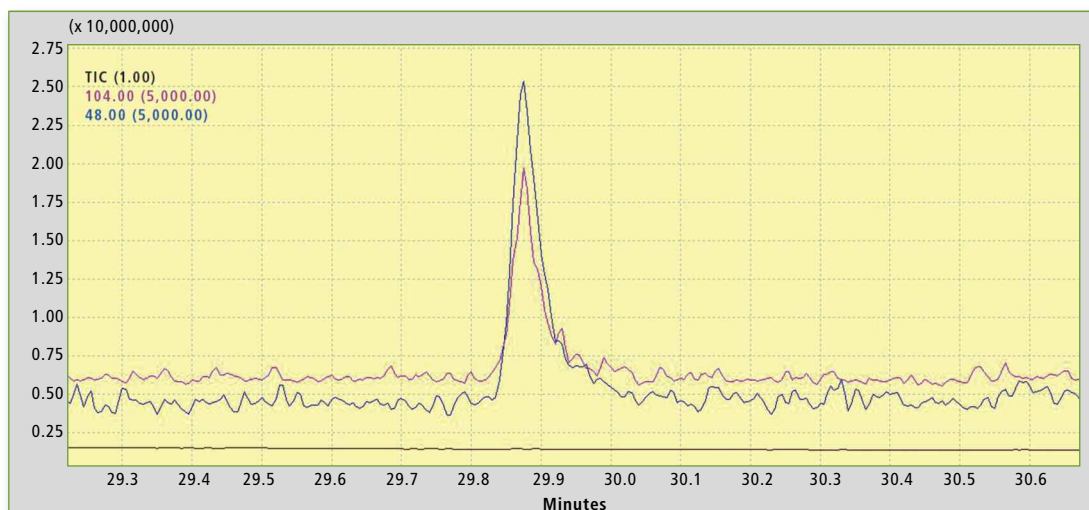
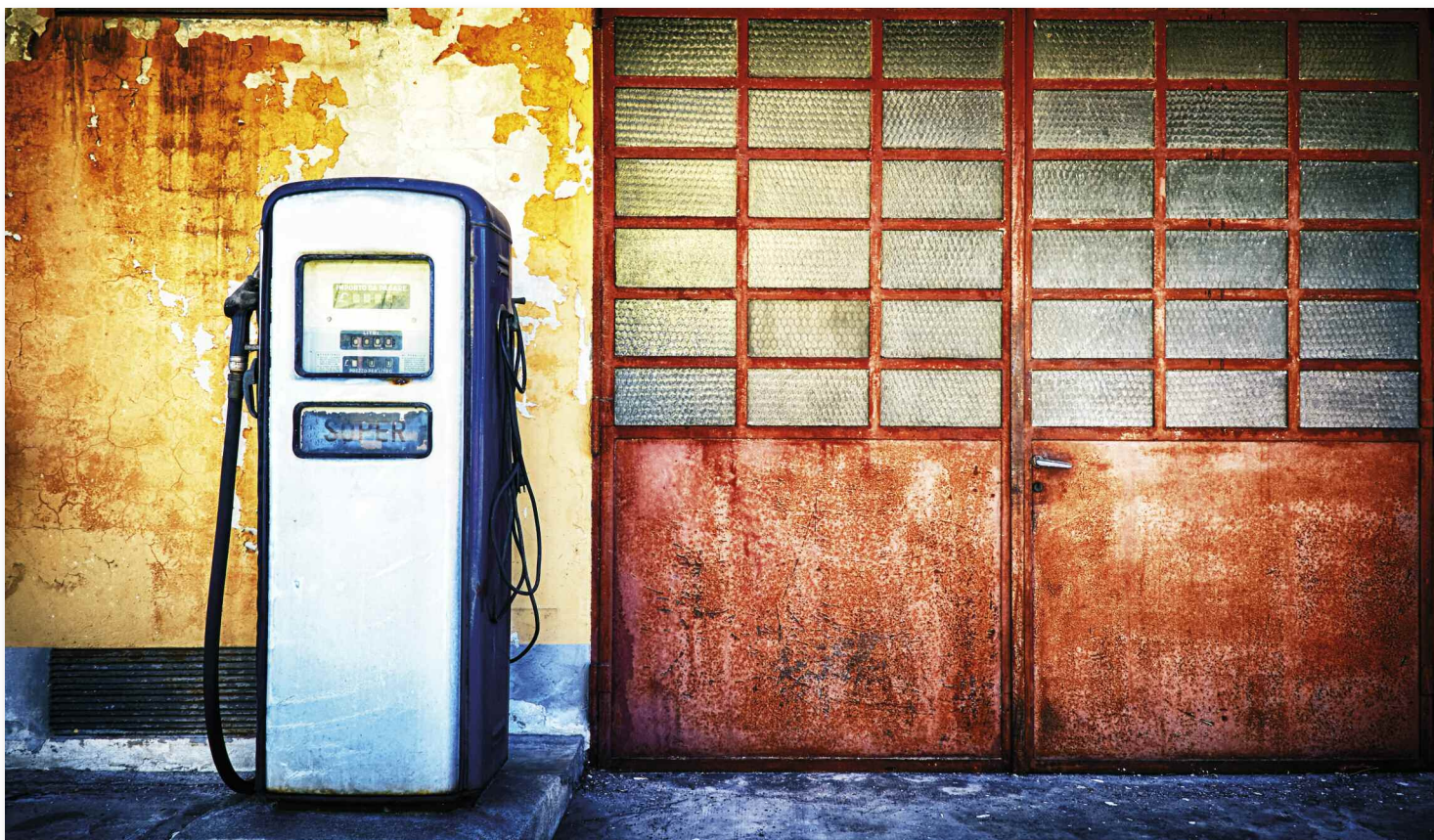


Figure 7: Identification of methional after heart-cut and separation on second column



Monitoring of total aromatics in gasoline

GCMS-QP2020 applied to ASTM D5769-04



In 1990, the American Congress amended the Clean Air Act, mandating the Environmental Protection Agency (EPA) to introduce reformulated gasoline with lower aromatics in polluted areas. This helped reduce vehicle emissions of toxic and ozone-forming compounds [1].

$$R = \frac{2(t_2 - t_1)}{1.699(y_2 + y_1)}$$

Figure 1: Calculation formula for resolution

Certifying that a fuel complies with the standards for reformulated gasoline requires monitoring of

its emission performance, calculated using equations derived from the “Complex Model” mandated after January 1, 1998. It requires input of a number of fuel parameters, one of which is the total aromatics content of the fuel. A standard test method was therefore developed by petroleum industry

scientists and adopted by the ASTM as ASTM D5769 [1]. In this standard, 23 known aromatic compounds are monitored while provisions are made for unknown aromatics which may be present in the sample [2].

Instrumentation, method parameters and sample preparation

Gas Chromatograph / Mass Spectrometer:
Shimadzu GCMS-QP2020 with AOC-20i Split/Splitless Injector

Capillary column:
MEGA-1 MS, 60 m x 0.25mm, 1 μm, part number: MS-1-025-10-60

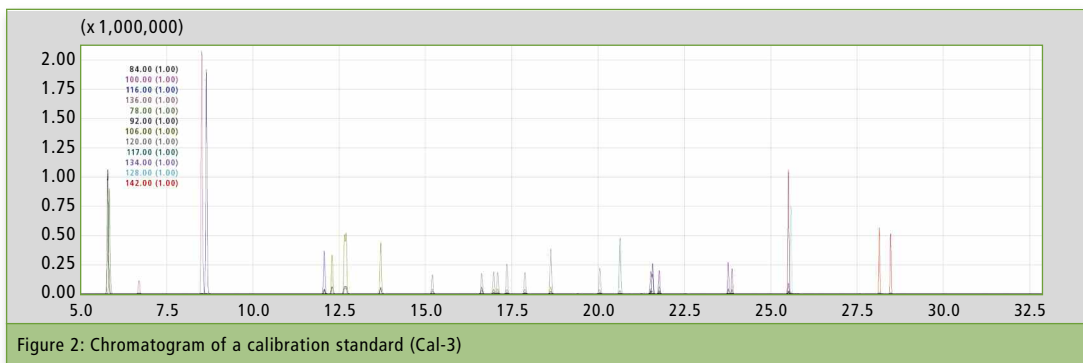


Figure 2: Chromatogram of a calibration standard (Cal-3)

Analytical method parameters are described in tables 1 and 2. With respect to sample preparation, the sample container was chilled upon reception in the laboratory, after which 1.0 mL of gasoline was transferred to a 1.8 mL vial. 120 μ L of internal standard mixture were subsequently added. Both masses were recorded to calculate the exact %w/w concentrations of the internal standards in the test solution and the dilution that the sample underwent upon addition of the internal standard amount.

ASTM D5769-04 acceptance criteria

The standard enforces strict acceptance criteria to ensure the quality of the results. Acceptance criteria were divided into four categories: Calibration curve, Gas Chromatography/Mass Spectrometry, QC sample, unknown samples.

Calibration curve:

1. A multipoint calibration curve consisting of at least five levels should be obtained.

2. For toluene, at least three points of the calibration curve should be higher than 50 % of the concentration range.
3. Deuterated analogs of benzene, ethylbenzene and naphthalene should be used as internal standards.
4. $r^2 \geq 0.99$ for the calibration curves of all compounds.

Gas Chromatography/Mass Spectrometry

1. Resolution between the peaks of 1,3,5-trimethylbenzene and 1-methyl-2-ethylbenzene each at the mass of 3 % level should be equal to or greater than 2.0. Resolution should be calculated according to the formula presented in figure 1 (page 25), where:

R = Resolution

t_2 = Retention time of 1,3,5-trimethylbenzene

t_1 = Retention time of 1-methyl-2-ethylbenzene

y_2 = Peak width at half height of 1,3,5-trimethylbenzene

y_1 = Peak width at half height of 1-methyl-2-ethylbenzene

Analyte	RT (min)	Least squares model	Correlation coefficient (r^2)
Benzene	5.8	Linear	0.998
Toluene	7.8	Quadratic	0.997
Ethylbenzene	10.0	Linear	0.997
1,3-dimethylbenzene	10.2	Linear	0.998
1,4-dimethylbenzene	10.2	Linear	0.996
1,2-dimethylbenzene	10.8	Linear	0.997
1-methylethylbenzene	11.6	Linear	0.998
Propylbenzene	12.4	Linear	0.995
1-methyl-3-ethylbenzene	12.6	Linear	0.998
1-methyl-4-ethylbenzene	12.7	Linear	0.999
1,3,5-trimethylbenzene	12.8	Linear	0.998
1-methyl-2-ethylbenzene	13.2	Linear	0.998
1,2,4-trimethylbenzene	13.5	Linear	0.997
1,2,3-trimethylbenzene	14.3	Linear	0.997
Indan	14.7	Linear	0.998
1,4-diethylbenzene	15.1	Linear	0.995
n-butylbenzene	15.1	Linear	0.997
1,2-diethylbenzene	15.3	Linear	0.999
1,2,4,5-tetramethylbenzene	16.8	Linear	0.999
1,2,3,5-tetramethylbenzene	16.9	Linear	0.996
Naphthalene	18.6	Quadratic	0.999
2-methyl-naphthalene	21.5	Linear	0.999
1-methyl-naphthalene	21.9	Linear	0.999

Table 3: Regression data

GC Parameters	
Column oven temperature	60 °C
Injection temperature	250 °C
Injection mode	Split
Split ratio	250 : 1
Injection volume	0.2 μ L
Sampling time	1.5 min
Flow control mode	Linear velocity
Column flow	1.5 mL/min
Linear velocity	35 cm sec ⁻¹ at 50 °C
Analysis time	33 min
MS Parameters	
Ion source	250 °C
Interface	280 °C
Solvent cut time	5 min
Acquisition mode	Scan
Interval	0.5 sec
Acquisition	5 - 33 min
Scan range	45 - 300 amu
Scan speed	500 amu/s

Table 1: Method parameters for GC-MS

Rate	Final temp	Hold time
—	60.0	0.0
3.0	120.0	0.0
10.0	250.0	0.0

Table 2: Gradient program

2. The system should be able to analyze repeatedly 0.01 % w/w 1,4-diethylbenzene with a Signal-to-Noise ratio of at least five.

3. Scan speed should ensure at least five spectra in the FWHM for the peak of toluene at 1-3 %.

4. A standard containing 1,2,3-trimethylbenzene (3 % w/w) should be injected, and the following relative intensities should be obtained: m/z 120: 30-60, m/z 105: 100, m/z 91: 7-15.

QC sample

A synthetic quality control mixture should be used to monitor the performance of the calibrated GCMS system. This QC sample should contain eight analytes in the levels described in table 5.

Apart from the analytes, the QC sample should also contain the following solvents: hexane (12 % w/w), heptane (17 % w/w), octane (17 % w/w), decane (12 % w/w), dodecane (5 % w/w) and 2,2,4-trimethylpentane (12 % w/w). The QC sample should be analyzed before each batch of samples.

Unknown samples

1. Relative intensities of the monitored ions should comply with the acceptance criteria described in table 5, when compared to the values obtained for a calibration standard containing the compound at approximately the same concentration.
2. Retention time at the maximum intensity scan should be within ± 15 s of the retention time of the respective calibration standard.

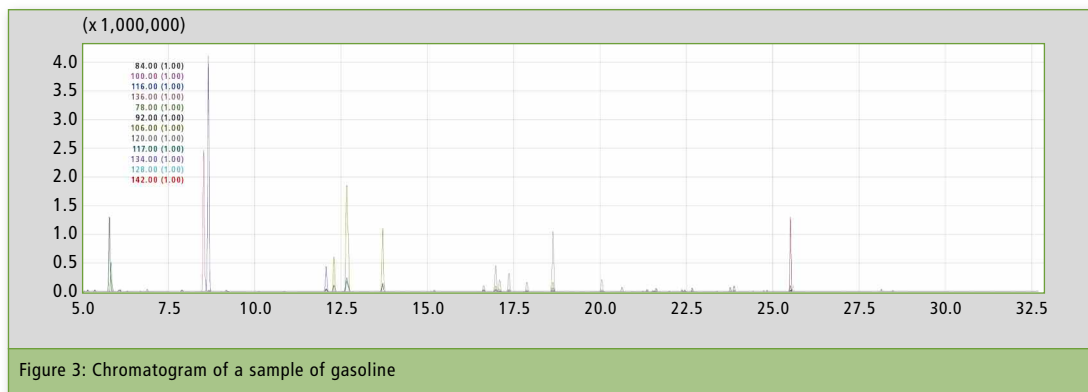


Figure 3: Chromatogram of a sample of gasoline

Results and discussion

A six-point calibration curve was obtained for all compounds, and one QC sample and one unknown sample were injected once. Acceptance criteria for the calibration curve, the GC-MS, QC sample and unknown sample were fulfilled. The chromatograms of a calibration standard and a sample of gasoline are presented in figures 2 (page 25) and 3.

Calibration curve

1. A multipoint calibration curve with six levels was obtained for each compound.
2. For Toluene, three points of the calibration curve were higher than 50 % of the concentration range.
3. Benzene d6, ethylbenzene d10, naphthalene d8 and toluene d8 were used as internal standards
4. r^2 was >0.995 for all compounds, as shown in table 3

Analyte	Concentration (% w/w)	Acceptance criteria for % error
Benzene	1	± 5
Toluene	9	± 5
1,3-dimethylbenzene	3	± 5
1,2-dimethylbenzene	3	± 5
Ethylbenzene	3	± 5
1,2,4-trimethylbenzene	3	± 5
1,2,4,5-tetramethylbenzene	2	± 10
Naphthalene	1	± 10
Total aromatics	25	± 5

Table 4: Composition and acceptance criteria for the QC sample

Gas Chromatography/Mass spectrometry

1. Resolution between the two peaks at the mass of 3 % level was 3.5 (Specification: >2.0).
2. Signal-to-Noise ratios of 175.1 and 230.8 were obtained for 1,4-diethylbenzene 0.01 % w/w at m/z 134 (Specification: >5)
3. Scan speed ensured six spectra in the FWHM for the peak of toluene 1-3 %.
4. The following relative intensities were obtained: m/z 120: 47.3 (Specification: 30 - 60),

m/z 105: 100 (Specification: 100), m/z 91: 8.0 (Specification: 7- 15).

QC Sample

1. Accuracy of results is shown in table 6.

Conclusion

1. Relative intensities of the ions monitored complied with the acceptance criteria described in table 5.
2. Retention time at the maximum intensity scan was within ± 15 s of the retention time of the respective calibration standard.

% Relative intensity	Acceptance criteria
> 50	± 30 %
20 - 50	± 50 %
< 20	± 100 %

Table 5: Acceptance criteria for the relative intensities of the ions monitored



Authors

Dr. Gerasimos Liapatas
Fotis Fotiadis
Georgia Flessia
Dr. Manos Barbounis
Applications Department of
N.Asteriadis S.A.
31 Dervenion Str. & Poseidonos Str., 144
51 Metamorfossi
Athens, Greece

Literature

- [1] M. Mathiesen, A. Lubeck, Improving accuracy in the determination of aromatics in gasoline by Gas Chromatography/Mass Spectrometry, J. Chromatogr. Sci. 36 (1998) 449 - 456. DOI 10.1093/ chromsci/36.9.449
- [2] D5769-04: Standard Test Method for the determination of benzene, toluene and total aromatics in finished gasolines by Gas Chromatography/Mass Spectrometry

Analyt	% Error	Acceptance criteria	Result
Benzene	5.0	± 5	Pass
Toluene	-2.4	± 5	Pass
1,3-dimethylbenzene	-2.2	± 5	Pass
1,2-dimethylbenzene	-4.6	± 5	Pass
Ethylbenzene	-1.0	± 5	Pass
1,2,4-trimethylbenzene	-2.4	± 5	Pass
1,2,4,5-tetramethylbenzene	4.7	± 10	Pass
Naphthalene	4.5	± 10	Pass
Total aromatics	-1.3	± 5	Pass

Table 6: Accuracy of results for the QC sample



Searching for the needle in the analytical haystack

Trace detection of sulfur compounds with SCD



Device image: Nexis GC-2030 with „SCD-2030 Sulfur Chemiluminescence Detection System“ and HS-20 Headspace Sampler

Combustion of sulfurous fossil fuels emits sulfur dioxide, which harms the human respiratory system and pollutes the environment through acid rain. In Europe, strict regulations and improved measuring tech-

niques have reduced this problem, but not eradicated it completely. For cost reasons, the petrochemical industry itself has a great interest in keeping sulfur compounds in the refinery process as low as possible in order to avoid

the destruction of expensive catalysts. Also in the food sector, sulfur compounds are an issue. In trace amounts they enrich flavor, but enjoyment is completely lost if the concentration is too high.

Challenge: Searching for clues in very complex samples

The challenge for analytical instrumentation is to detect traces of sulfur in very complex samples such as crude oil, food and beverages – a search for the needle in the analytical haystack. Sulfur-selective chemiluminescence detectors (SCDs) are a possible solution.

With the Nexis SCD-2030 Sulfur Chemiluminescence Detection System, Shimadzu presents a completely new solution. After client feedback, aspects such as easier handling and maintenance, long-term stability and automation have been implemented through extensive software integration during development.

Sulfur is detected by the chemiluminescent reaction of sulfur monoxide with ozone to form sulfur dioxide. Sulfur dioxide is produced for a very short time in the excited state. Excess energy is emitted as light (300 - 400 nm) and can be detected by a photomultiplier (PMT).

Complex detector scheme required for selective sulfur detection

The conversion of any sulfur compound to sulfur monoxide

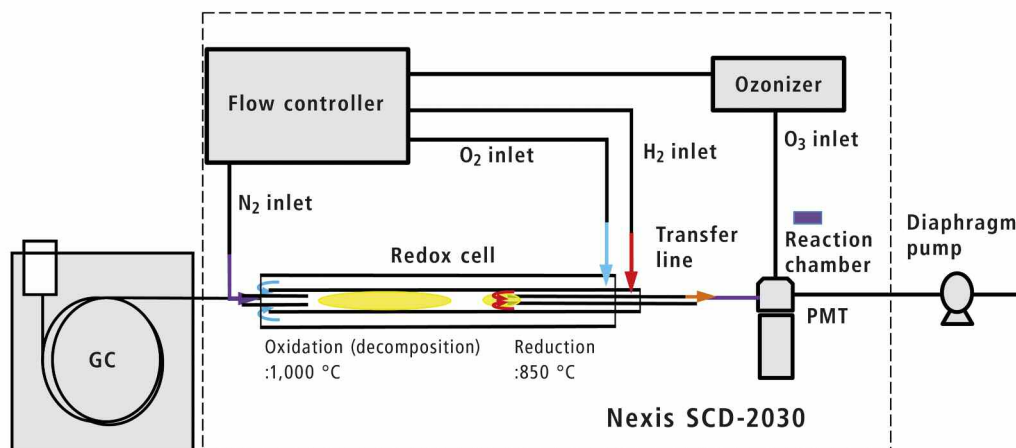


Figure 1: Schematic of the SCD-2030. After chromatographic separation in the GC-2030, components pass into the redox cell and from there to reaction chamber and photomultiplier (PMT).

requires various steps, which are processed in successive modules. The detector scheme of an SCD is correspondingly more complex than that of other GC detectors such as the flame ionization detector (FID).

The SCD-2030 detector scheme (figure 1) shows the course that the sample takes during measurement. From the GC column, all components first enter the redox cell. Ideally, everything is oxidized here at 700 - 1,000 °C by the addition of oxygen. In the subsequent step, the resulting sulfur dioxide is reduced by means of adding hydrogen to form sulfur monoxide.

The final chemiluminescence reaction of the sulfur monoxide with ozone should preferably not be disturbed by cross-sensitivities or unwanted reactions of the ozone. Ideally, in an SCD chromatogram, only signals of sulfur compounds can be seen.

An additional advantage is the equimolarity of the SCD to sulfur, which greatly simplifies the calibration. Equimolar signifies that with a compound of two sulfur atoms, the detector signal is twice as high compared to mono-sulfur compounds. Due to the high sulfur selectivity, the total sulfur content of a sample as well as the individual components can be determined after chromatographic separation.

Horizontally mounted redox cell increases long-term stability

Just how the ideal case is achieved depends in practice, among other things, upon the performance of the redox cell. If oxidation and reduction are not complete, this can lead to losses in terms of selectivity, reproducibility and ultimately sensitivity.

For this reason, Shimadzu has opted for a horizontally mounted redox cell in the SCD-2030 design. This allows for a much larger redox cell and the shortest possible connection to the subsequent reaction cell and the photomultiplier. The advantage of short paths and inert materials is the

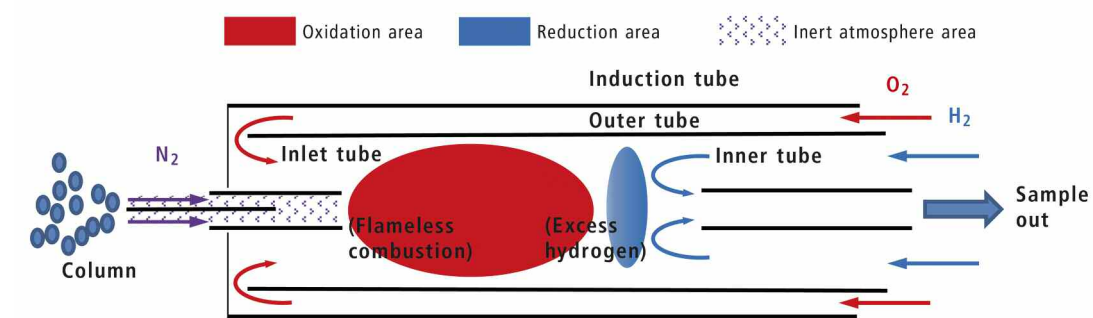


Figure 2: Schematic of the SCD-2030 redox cell. Eluents from the GC column are oxidized in the first step. Sulfur oxidizes to sulfur dioxide and is then reduced to sulfur monoxide in the subsequent step. Nitrogen is added as an inert „make-up“ gas

exceptional long-term stability of the SCD-2030.

Through a large redox cell, a longer residence time of the components is achieved, whereby the oxidation proceeds almost quantitatively even at high carrier gas flows. The resulting dynamic range eliminates the need for frequent fine tuning of all gas flows to maintain the efficiency of oxidation and subsequent reduction of sulfur dioxide.

Simplified maintenance

The „Inner Pyro Tube“ (figure 2 „Sample Out Page“) is a consumable part of the SCD that requires the most maintenance. Here, the horizontal design provides easy access and simplifies regular maintenance. The same applies to the „Outer Pyro Tube“, whose maintenance intervals are significantly longer.

Detection of sulfur components ultimately takes place in the reaction cell and the coupled photomultiplier. Ozone for the chemiluminescent reaction provides a generator via electrical discharge of pure oxygen. It is important to

prevent „electrical overcurrents“ to ensure a long life of the generator.

Overcurrents in the ozone generator are formed due to impurities in the oxygen. In order to prevent damage, a new arrangement with constant current and monitoring of the electrical voltage has been developed. Continuous monitoring and diagnostics warn early on of any malfunction. Reaction cell and detector of the SCD are operated under reduced pressure.

Due to the compact design, the SCD-2030 is equipped with a simple diaphragm pump.

When starting an SCD, all modules must be booted up in a defined sequence (figure 3). This can take over an hour. With the SCD-2030, this is fully automated. With extensive software control and internal monitoring capabilities, user intervention is not required. Within a sequence, predefined conditioning steps can also be inserted automatically. The SCD-2030 can also be shut down automatically after completion of a sample sequence. Since cooling of the over 700 °C hot redox cell takes some time, the automatic

shutdown saves longer waiting times in order to carry out planned maintenance work.

Summary

Selective detection of sulfur traces by means of chemiluminescence requires several reaction steps. Robust technology, new design for easy maintenance and high automation of the SCD-2030 detector make the complex technology accessible to the less experienced user.

Robust technology has been achieved with the SCD-2030 by changing to a horizontally installed redox cell. The larger dimensions allow a longer residence time of all components for maximum efficiency in the oxidation and reduction reactions.

This promotes selectivity and thus sensitivity to sulfur compounds. Combined with the short transfer line to the reaction cell and photomultiplier, this guarantees high long-term stability of the SCD-2030.

Consumables of the SCD-2030 (e.g. Inner Pyro Tube) are easily accessible, making maintenance easy and quick.

Comprehensive software control allows automated start and shut down of the detector and predefined condition procedures in case of contamination.



Figure 3: During automatic start-up, each module of the SCD-2030 is started up step by step. Interim intervention by the user is no longer required before readiness for measurement.



The glowing lemonade

Quantitative fluorescence analysis of quinine flavor in various preparations



Figures 1a and 1b: Bottles of tonic water under normal light conditions on the left, and a bottle showing fluorescence phenomenon

The classic of fluorescence spectroscopy, which almost everyone has seen, is a drink that glows in black light. This glow of tonic water or bitter lemon sodas can be attributed to quinine. Its luminosity, the fluorescence, is so intense that it can be used as a fluorescence standard.

What is quinine?

Chemically, it is an alcohol 1-(6-methoxyquinolin-4-yl)-1-(5-vinyl-1,4-ethanopiperidin-2-yl)methanol having the empirical formula $C_{20}H_{24}N_2O_2$. The corresponding structure shows a ring system with an aromatic part that is, among other things, the cause of fluorescence. In simple terms, the π electrons of the double bonds can be stimulated with a high-energy light source (short wavelength – UV radiation). With the energy absorbed, the electrons leave their energetic ground state and after a short time they return

to it, emitting the absorbed energy (fluorescence).

This white crystalline solid – quinine for short – was discovered in the 17th century as a medicine to treat malaria. Since that time, about 300 mg of quinine has been and continues to be used for a medical dose.

Historically, the colonialists working in malaria areas created „tonic“ water or „bitter lemon“ beverages to proactively protect from malar-

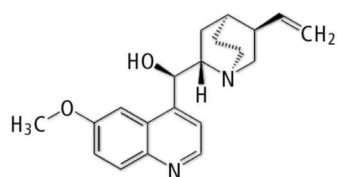


Figure 2: Sketch of the quinine structural formula

ia. These drinks are still offered today. For example, an average of

70 mg/L quinine is used for tonic water and 30 mg/L for bitter lemon.

Much like the taste of a grapefruit, quinine brings the bitter/harsh taste to the drink. Due to changes in consumer behavior, the self-production of beverages is a way for consumers to come into contact and work with quinine. This flavor, bottled in small vials, is available on the market.

Fluorescence behavior of quinine

In this application, it will be shown how the fluorescence behavior of quinine under different fluid environments can be changed and quantified.

Fluorescence spectroscopy is selective. A substance can be determined out of a mixture. Nevertheless, the environment of the mixture (here: solution) to

be determined needs to be taken into account. The fluorescence of liquids depends on the temperature, the concentration of the fluorophore, the solvent and the pH of the solution [1]. Bitter lemon and tonic water from the supermarket, declared as quinine-containing drinks, and a tonic water flavor for making sodas were analyzed.

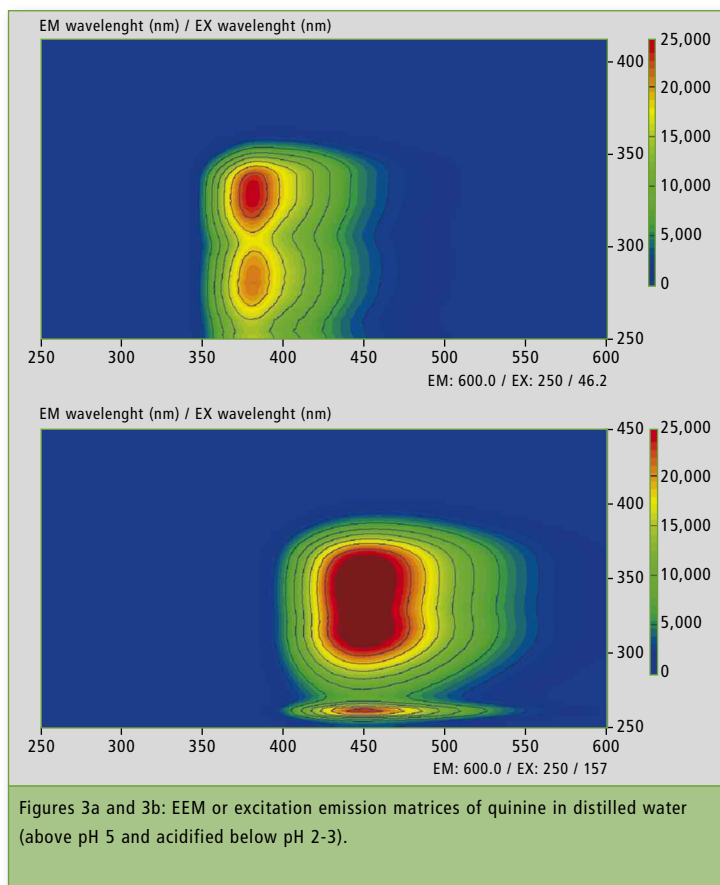
The tonic water flavor used is said to contain 6 % quinine, water, alcohol, aroma extract and natural flavors. Due to the high concentration of quinine, the flavor was diluted 1:50,000.

Influence of pH on the analytical wavelengths

As a reference material, chemically pure quinine was dissolved in distilled water. This solution had a pH of 5. By comparison, the carbonated acidified sodas have a

Intensity at EM 449 nm	Quinine [mg/L]
88.548	0.05
137.096	0.1
214.153	0.15
266.866	0.21
336.795	0.26
402.928	0.31
469.410	0.36
531.006	0.41
592.821	0.46
659.707	0.51
711.222	0.56
778.106	0.61
887.907	0.67
1,258.75	1.03
2,514.80	2.06
3,698.36	3.09
4,858.05	4.12
5,935.70	5.15
10,652.5	10.3
14,746.9	15.45
18,824.2	20.59
21,649.0	25.74

Table 1: 22 standards prepared from acidified quinine solutions, concentrations and fluorescence of the analytical wavelength pair



Figures 3a and 3b: EEM or excitation emission matrices of quinine in distilled water (above pH 5 and acidified below pH 2-3).

pH of 2-3. In this experiment, the tonic water flavor was mixed once with distilled water (pH 5) and once with water acidified with sulfuric acid (pH 2-3). Measurements were taken on the Shimadzu RF-6000 Fluorescence Spectrophotometer with a standard fluorescence-free cuvette.

Both solutions were characterized by the fluorescence measurement. For comparison, the solutions were measured in an EEM (Excitation Emission Matrix), where the fluorescence-active regions are recognized. With the same scaling, it is obvious that the acidified matrix is shifted towards the long-wavelength range. At pH 5, the analytical wavelength pair (excitation/emission) is 275/375 (region 1) and 325/375 (region 2) nm, and shifts at pH 2-3 to 325/450 (region 1) and 350/450 (region 2) nm. The influence of pH on the

excitation and emission of fluorophores is known [1].

Quinine content checked

To check the quinine content, a calibration series of 22 standards (table 1, acidified, pH 2-3) was prepared, covering a wide concentration range (0.05 to 25.74 mg/L) with the same measurement parameters (excitation at 345 nm and emission at 449 nm). Figure 4 shows the calibration curve of the experiment.

The fluorescence intensity of the standards at 449 nm and their quinine concentration can be connected by a polynomial calibration curve of the second degree. The compensation calculation gives a correlation of 0.9997, where 1 would be the ideal state. This calibration was chosen to

demonstrate the dynamic range of the device.

For analysis, conventional sodas in PET bottles from various suppliers as well as one flavoring were obtained. Exemplary measurements with tonic water and the tonic water flavoring are shown.

In order to demonstrate the selectivity of the fluorescence and the dynamic range of the device, a variety of dilutions were used. In the case of the tonic water flavor, the measured intensity and the ensuing calculated concentration of about 55 g/L correlates with the information provided on the bottle (6 % quinine corresponds to an amount of 60 g/kg). For the brand-name lemonade, the measured intensity and the subsequently calculated concentration of about 77 mg/L correlates with

reliably with this method. A calibration from low to high concentration can be made with quinine and could be carried out without changing the measurement parameters with respect to detector sensitivity and grating adjustment. An optimization of the calibration can be achieved by smaller concentration ranges and adapted device parameters.

Literature

- [1] Principles of Fluorescence Spectroscopy, J.R. Lakowicz, 3rd Edition, 2010, Springer
- [2] Aromaverordnung, <https://www.gesetze-im-internet.de/aromv/BJNR016770981.html>

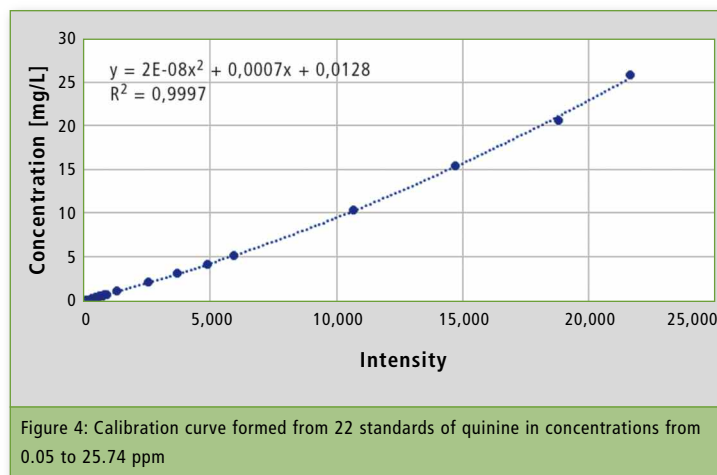


Figure 4: Calibration curve formed from 22 standards of quinine in concentrations from 0.05 to 25.74 ppm

the information found in the literature (about 70 mg/L quinine). By comparison, quinine in the discount goods was less well-dosed. Both lemonades fulfill the permitted quinine concentrations according to the flavor regulation [2], because they are below the limit of 85 mg/L.

Conclusion

Quinine in lemonade and flavoring concentrate can be determined

Sample	EM 449 nm	Conc. [mg/L]	Dilution factor	Quinine (mg/L)	Manufacturer's information
Concentrate - flavour tonic water	1,485	1.10	50,000	54,835.94	6 % (~60 g/L) quinine in solution
Branded goods - tonic water	1,056	0.77	100	77.43	~70 mg in drinks
Discount goods - tonic water	2,680	2.03	25	50.82	

Table 2: List of samples, their dilution, fluorescence intensity and calculated quinine content

Recognized for outstanding designs

iF DESIGN AWARD 2019 for time-of-flight mass spectrometer

More than 2,000 guests from 42 countries: in Mid-March, the prestigious international iF DESIGN AWARD ceremony was held in the BMW Welt event venue in Munich, Germany. Shimadzu's Q-TOF LCMS-9030 time-of-flight mass spectrometer was one of the prize-winning units.

The iF DESIGN AWARD has long become a symbol for excellent form, for aesthetic quality, and for user-focused, ergonomic and efficient design in all disciplines, by companies around the world. It is based on the decision of an independent jury of 67 experts from 20 countries.

The iF Design Award is donated by the Germany-based iF Industrie Forum Design organization which is joined by other design professional organizations around the world to increase public awareness about design. For this year's award, nearly 6,400 entries from 50 countries applied.

The LCMS-9030 has been awarded in the Industry/Tools category. This research grade mass spectrometer provides accurate mass detection with incredibly fast data acquisition rates, allowing scientists to identify and quantify more compounds with greater confidence. It targets



Ms. Hyeri Kang, the designer of the Q-TOF LCMS-9030, accepted the award at the iF DESIGN AWARD night 2019 in Munich

environmental, forensic medicine, foods and life sciences applications.

Particularly in B2B environments, efficient as well as ergonomic and user-friendly features are decisive for systems in daily use. In the last seven years, Shimadzu systems have been recognized three times with an iF DESIGN AWARD.

Coming next

Shimadzu has also been awarded two Red Dot Design Awards 2019 for its new Nexera UHPLC series LC-40 and the UV-1900 UV-Vis spectrophotometer. The next issue of the Shimadzu-News edition will cover the Red Dot Award Ceremony 2019 taking place in July.

Shimadzu live

TIAFT
Birmingham,
Great Britain
September 02-06, 2019
www.tiaft2019.co.uk/

Composite
Stuttgart, Germany
September 10-12, 2019
www.composites-europe.com/de/

PBA
Tel Aviv,
Israel
September 15-18, 2019
www.pba2019.org/

MSACL
Salzburg, Austria
September 24-26, 2019
www.msacl.org/

CANAS
Freiberg, Germany
September 23-26, 2019
www.tu-freiberg.de/canas

VLB Oktobertagung
Berlin, Germany
October 14-15, 2019
www.vlb-berlin.org/okt2019



@ShimadzuEurope

NEWS – print and digital



Print version: If you would like to receive the Shimadzu News on a regular basis, please email us your postal address via: shimadzu-news@shimadzu.eu



Also as App: the Shimadzu NEWS is also available as WebApp via www.shimadzu-webapp.eu



You can also subscribe to our newsletter via: www.shimadzu.eu/newsletter